Università degli Studi di Napoli FEDERICO II
Polo delle Scienze e delle Tecnologie
Facoltà di Ingegneria
Dipartimento di Ingegneria Elettrica

Tesi di Dottorato di Ricerca in Ingegneria Elettrica

Identification of Broadband Passive Macromodels of Electromagnetic Distributed Structures

by

Luciano De Tommasi

Coordinator: Prof. Guido Carpinelli

Supervisor: Prof. Massimiliano de Magistris

Napoli, 2006

Contents

Acknowledgements

I would like to thank all the people who supported and encouraged me during my Ph.D. studies.
First of all, I would like to give my special thanks to Prof. Massimiliano de Magistris, who have been the responsible for all my research program. I guess that without his help this dissertation would have been confusing and hard to read.
I wish to express my gratitude to Prof. Antonio Maffucci for several stimulating discussions on transmission line theory and modelling and for his help in writing part of this dissertation.
Thanks to Dr. Bjorn Gustavsen, who offered me an invaluable research experience at SINTEF Energy Research AS, Trondheim (Norway). He taught me several things regarding the reduced order modelling of power systems, and also to be more concrete as an engineer should be.
Thanks to all the staff of SINTEF Energy Research AS, for their kind hospitality and for the stimulating environment.
Dr. Massimo Nicolazzo provided a timely assistance with the LaTeX environment that I did not know in detail.
Prof. Giovanni Miano, as early coordinator of the Ph.D. in Electrical Engineering, provided a stimulating educational environment with many interdisciplinary courses and seminars.
Thanks to Prof. Guido Carpinelli for his kindness and availability, and for having taken on the role of coordinator of the Ph.D. in Electrical Engineering in the last period of my studies.
Last but not least, thanks to my colleagues and friends Walter, Massimiliano, Andrea and Dario, who shared with me their knowledge, providing help and support when needed.

Introduction

The issue of macromodelling has received a great attention in these last years, mainly due to increasing speed and decreasing size of electronic circuits, which makes critical the accurate modelling of passive structures and interconnects. On the other hand, also power systems do require accurate macromodels to implement transient simulations.

The derivation of a reduced order model may be either needed to implement fast time domain simulations or the unique possibility to include a certain component in a circuital simulator, when it can be only characterized by measurements. First case includes transmission line simulation, and macromodelling of structures characterized through full-wave electromagnetic simulations. Instead a typical example of the second possibility is the transformer modelling.

From a general point of view, when describing operators of a physical model can be written as rational function, this particular structure may be exploited to handle them in a more efficient manner. A typical example is the possibility to introduce the recursive convolutions instead of "slow" convolutions, which leads to a more efficient implementation of a time domain scheme. On the other hand, there are complex real systems which cannot be satisfactorily characterized by physical models with known few parameters, so requiring a characterization through measurements. In such cases, the derivation of a reduced order model makes possible the analytic description of the system, which corresponds to the extraction of a lumped circuit equivalent.

The key-point of the macromodelling approach is the identification of a lumped equivalent. In the frequency domain, this corresponds to a rational approximation of tabulated transfer functions. Several algorithms for this purpose have been studied in the last fifty years, and successfully applied in several branches of electrical engineering. The problem is even more general than the scope of the present work, which is limited to the model order reduction of electromagnetic distributed structures with the purpose of performing time domain analyses.

Despite to its apparent simplicity, the mathematics of the algorithms for rational approximation of frequency responses has not been yet deeply understood from a theoretical point of view. Iterative algorithms are given without a theoretical under-

standing of their convergence properties and initialization. On the other hand, best approaches are very recent.
Second fundamental issue is the imposition of physical requirements for the macromodel. Whereas the stability of a macromodel can be easily controlled, requiring passivity is often much more delicate. When rational functions are used to approximate transfer functions of passive structures, they also should represent a passive circuit. This is not immediately related to the accuracy of the approximation performed: even good approximations of passive systems may exhibit a non-passive behaviour. Furthermore, passivity constraints are impractical to be included in the identification stage, therefore they are usually enforced in a subsequent stage. On this point, there exists several approaches which gives quite good results, but literature shows a lack of a deep comparison among them. Algorithms for passivity enforcement have been mainly developed referring to specific applicative contexts, and their effectiveness mainly validated on the same kind of datasets.
This work is divided in four chapter.
Chapter 1 starts with a unified and synthetic description of the problem of identification of a rational approximation for a multi-input multi-output electromagnetic system. Therefore, a new algorithm for the identification of a magnitude frequency response with a minimum phase shift function is given. This is an useful tool either when measurements include only magnitude responses or when it is convenient to ignore the information provided by the phase angle. Moreover, a new robust approach to identify accurate macromodels with state space realization without pole repetitions is shown. Examples of application to interconnects modelling are included.
Chapter 2 reviews the black-box identification (i.e. the identification ignoring any information provided by a known physical model) and passivity enforcement algorithms. Then, the application of known algorithms to macromodelling of a twisted cable previously characterized through a full-wave simulation, is presented.
Chapter 3 describes the simulation of transmission lines and related issues of macromodelling. Approaches coming from both interconnects and power lines are compared.
Regarding the interconnects modelling, a new definition of the regular part of a describing operator of the line is given. This is combined with the identification technique given in chapter 1, leading to an improved approach with respect to those available in literature.
Therefore, the magnitude fitting algorithm introduced in chapter 1 is successfully exploited to give a new procedure of identification including time delays of the line. Its effectiveness is validated on overhead transmission line datasets, and its limitations pointed out.
Chapter 4 includes the validation of described approaches through time domain analyses exploiting reduced order models. Furthermore, the black-box modelling approach is successfully applied to an important class of "high speed" interconnects.

Chapter 1

The identification of reduced order models

1.1 Introduction

There are quite a number of electrical and electronic systems, in different technological contexts, where typically a distributed passive electromagnetic structure interacts with lumped elements (possibly non linear). Normally their "system level" analysis and design is based on circuit simulation. There is therefore the need of determining reduced models for the distributed structures that can be efficiently and easily integrated in circuital simulators, after direct measurements or full wave simulations are available. Some examples quite recently explored can be found in the high frequency modelling of electrical power systems, as well as in the modelling of "high speed" interconnects in electronics.
The technological pressure toward high speed devices requires that the reduced models should be accurate in extremely large frequency intervals. Moreover, those distributed structures are intrinsically passive, and this property has to be preserved in the process of finding the reduced models in order to get guaranteed stable simulations. All those requirements make the identification of broadband passive macromodels not a trivial problem, and this reflects into the effort of some recent literature.
Considering the general case of multi-input-multi-output structures, the frequency domain lumped equivalent macromodels can be derived through the identification of a proper rational approximation of the transfer matrix. This identification can be pursued with a "black box" approach, which reveals to be easy and efficient in many cases. Better results, in terms of either low order or high accuracy, can be often obtained with a "grey box" approach, where structural properties provided by a known physical model are exploited to define regular describing operators to be identified.
Recent literature has shown with clear evidence that, among many proposed schemes,

an iterative algorithm named *Vector Fitting* (VF) is by far the most robust and efficient presently available. Its performances are adequate to most practical cases of black-box and gray-box modelling. It is a linear algorithm which identifies a transfer function through an iterative process of poles relocation. This involves two steps: the identification of poles and the identification of residues. Each of them is solved by formulating a linear least square problem.
Since the basic idea of poles relocation has shown to be very effective, there is a great interest in literature around the VF algorithm, in the perspective of adding new features and/or further improvements.
In this chapter, after giving a unifying description of the most known identification ideas, some original results concerning the identification through the VF algorithm will be given. They are namely:

- a new formulation able to identify a tabulated magnitude frequency response through a minimum phase shift rational function;

- a non-linear identification process eliminating pole repetitions appearing in the state space realization previously identified by means of the VF algorithm.

1.2 Rational approximation of frequency domain responses

The identification of frequency domain responses of distributed systems with rational approximations is a quite old problem, which has been originally addressed in the area of automatic control (Levy 1959 [1], Sanathanan and Koerner 1963 [2]). That primary effort has been further developed in the area of filters synthesis and optimal design, (e.g. Shaw 1995 [3]).
Nowadays the problem of describing electromagnetic distributed structures through reduced order models is even more widespread, and in addition with heavy requirements in terms of bandwidth in most application contexts. For this reason, recent literature has given some effort to the subject, and satisfactory solutions are now available. As already mentioned the VF algorithm [4], has distinguished for its good properties and is now considered as the reference standard in the field.
The identification of a rational transfer function starting from a tabulated frequency response leads to a straightforward derivation of an equivalent circuit. This is a very interesting possibility, for instance in the filters synthesis. Furthermore, the derivation of time domain models is straightforward too.
Let us briefly recall such an implementation scheme of the time domain model. When a system is described through its transfer function $F(s)$, the relation between the input $U(s)$ and the output $X(s)$ is:

$$X(s) = H(s) \cdot U(s), \tag{1.1}$$

which corresponds in the time domain to:

$$x(t) = h(t) * u(t) = \int_o^t f(t-\tau)u(\tau)d\tau. \tag{1.2}$$

The practical implementation of (1.2) needs to discretize the convolution integral. For simplicity we assume a constant time step Δt and set $x(n \cdot \Delta t) = x_n$. Such a discretization also highlights the possibility of a recursive evaluation of the convolution integral (1.2):

$$x_n = \int_o^{(n-1)\Delta t} h(t-\tau)u(\tau)d\tau + \int_{(n-1)\Delta t}^{n\Delta t} h(t-\tau)u(\tau)d\tau =$$

$$= x_{n-1} + \int_{(n-1)\Delta t}^{n\Delta t} h(t-\tau)u(\tau)d\tau. \tag{1.3}$$

When $H(s)$ is a rational function, the recursive formula (1.3) can be further developed, giving:

$$x_n = \alpha u_n + \beta u_{n-1} + \gamma x_{n-1} \tag{1.4}$$

where coefficients α, β and γ can be evaluated with different methods, so giving different formulas (e.g. Gustavsen et al 1999 [5]).
For the general case of multi-input multi-output system (MIMO), the identification problem could be cast in the following form: let us consider to know (both from full wave simulations or direct measurement) a series of N_s samples $\{H_k = H(s_k)\}_{k=1....N_s}$ of the $m \times m$ complex matrix frequency response $H(s)$. The matrix function $H(s)$ can be then approximated by means of the expansion:

$$\tilde{H}(s) = \frac{\sum_{i=1}^{M} R_i f_i(s)}{\sum_{j=1}^{N} a_j g_j(s)}, \tag{1.5}$$

where $\tilde{H}(s)$ and $\{R_i\}$ are $m \times m$ matrices, $\{a_i\}$ are scalar values and $\{f_i\}$, $\{g_j\}$ are generic basis functions, N is the expansion order, and the numerator degree M has to satisfy $M \leq N + 1$.
Once some basis function has been chosen, the identification of $\{a_i\}$ and $\{R_i\}$ is a classical least square problem that can be set as the minimization of the cost function:

$$\chi(\{R_i\},\{a_j\}) = \sum_{k=1}^{N_s} \left\| H(s_k) - \frac{\sum_{i=1}^{M} R_i f_i(s_k)}{\sum_{j=1}^{N} a_j g_j(s_k)} \right\|_F^2, \tag{1.6}$$

where with the notation $\|.\|_F^2$ we indicate the Frobenius norm*.
Since a rational approximation directly corresponds to a lumped system (which is the ultimate goal for reduced models), the most immediate choice for the basis function is:

$$f_i = s^{i-1} \quad g_j = s^{j-1} \tag{1.7}$$

1.2.1 Rational approximation through nonlinear identification

Expression (1.6) is non-linear dependent from $\{a_j\}$ parameters, therefore that minimization problem can be immediately addressed using a non-linear least square algorithm, for instance Levenberg-Marquardt or Gauss-Newton (e.g. Fletcher [6]).
The identification of a transfer function:

$$\tilde{H}(s) = \sum_{i=1}^{N} \frac{R_i}{s - p_i} + D \tag{1.8}$$

is carried out by minimizing the cost function:

$$\chi_{NLLS}(\{R_i\}, D, \{p_i\}) = \sum_{p=1}^{m} \sum_{q=1}^{m} \sum_{k=1}^{N_s} \gamma_{pqk} \left\| H_{pq}(s_k) - \tilde{H}_{pq}(s_k) \right\|^2, \tag{1.9}$$

which generalizes the (1.6), allowing the most general weighting of the matrix $H(s)$ under identification.
Note that smooth functions, such as the operators describing long interconnects (see chapter 3) can be easily identified with a nonlinear approach constraining the poles to be real. This does not degrade the accuracy whereas adds robustness to the identification process, also simplifying the subsequent implementation of the time domain simulation.
The main drawback of such an approach is that the NLLS can stop in local minima of (1.9), so limiting the accuracy of the identification.
However, the advantages of a nonlinear identification can be usefully exploited, when a good starting guess is previously obtained by using a linear method.

1.2.2 Rational approximation through linear identification

The identification problem (1.9) can be linearized recasting it as the minimization of the "weighted" function:

$$\widehat{\chi}(\{R_i\}, \{a_j\}) = \sum_{k=1}^{N_s} \left\| H_k \sum_{j=1}^{N} a_j g_j(s_k) - \sum_{i=1}^{M} R_i f_i(s_k) \right\|_F^2. \tag{1.10}$$

*The Frobenius norm, sometimes also called the Euclidean norm, is a matrix norm of an $m \times n$ matrix A defined as: $\|A\|_F = \sqrt{\sum_{i=1}^{m} \sum_{j=1}^{n} |a_{ij}|^2}$. It is also equal to the square root of the matrix trace of AA^H, where A^H is the conjugate transpose of A: $\|A\|_F = \sqrt{Tr\,(AA^H)}$.

Algorithms based on the idea of minimizing (1.10) assuming the basis function (1.7), are, for example, the Model Based Parameter Estimation (MBPE) (Brittingham et al. 1980 [7]) or the Rational Function Approximation (RFA) (Gao et al 2005 [8]).
The minimization of (1.10) gives rise to large errors if the identified poles of $H(s)$ gives wide variations to the factor $\sum_{j=1}^{N} a_j g_j(s_k)$ throughout the considered set of frequency samples. An iterative method which removes this biasing from (1.10) can be established as follows. After a first iteration where expression (1.10) is minimized, a new cost function is considered as:

$$\breve{\chi}(\{R_i\}^{(n+1)}, \{a_j\}^{(n+1)}) = \sum_{k=1}^{N_s} \left\| \frac{H_k \sum_{j=1}^{N} a_j^{(n+1)} g_j(s_k) - \sum_{i=1}^{M} R_i^{(n+1)} f_i(s_k)}{\sum_{j=1}^{N} a_j^{(n)} g_j(s_k)} \right\|_F^2, \tag{1.11}$$

which is expected to approach (1.6) as the number of iteration n increases. The advantage of introducing the cost function (1.11) is that it is still linear as (1.10) and, at the same time, it is similar to (1.6), since the factor originally eliminated in (1.10) has been restored, although evaluated at the previous iteration. This method is known as Sanathanan-Koerner (SK) algorithm [2].
It is crucial to observe that the assumption (1.7) gives severe limitations to the contemporary increase of the order of the approximation and the bandwidth of the system under identification, since high powers of s lead to numerically ill conditioned matrices in the solution of (1.10) and ((1.11)). In other words, position (1.7) is possible as long as the systems under identification are well approximated with low order expressions and/or they need to be described only in limited frequency ranges.
The Vector Fitting (VF) algorithm [4], originally developed independently from the SK scheme, has been recently recognized as a specific reformulation of it (Hendrickx and Dhaene 2006 [9]). It is, in fact, a particularization of the scheme (1.11) with the use of the simple fraction as basis functions:

$$\begin{cases} f_i = \dfrac{1}{s - p_i} & i = 1, \ldots, N-2; f_{N-1} = 1; f_N = s; \\ g_i = \dfrac{1}{s - p_i} & i = 1, \ldots, M-1; g_M = 1. \end{cases} \tag{1.12}$$

The terms f_{N-1}, f_N can be conveniently modified according the asymptotic behavior (i.e. $s \to \infty$) of the function under identification. We set $f_{N-1} = f_N = 0$ when it vanishes, and $f_{N-1} = 1$, $f_N = 0$ when it approaches a constant value. Actually, the base function $g_M = 1$ was not used in the original version of the algorithm, described by Gustavsen and Semlyen in [4]. Gustavsen (2006) [10], has shown that this additional degree of freedom in the solution of the linear least

square problem, improves the convergence properties.
Note that this choice of the basis function removes to a large extent the ill conditioning of the problem for wide frequency intervals.
Actual implementation of VF [4] will be discussed in section (1.4). The relaxed formulation [10] will be exploited in a modified formulation of VF suitable for the identification of magnitude frequency responses, described in the section (1.5.2).
Now, let us just observe that by substituting the basis functions (1.12) into equation (1.11), we get as denominator:

$$\sigma^{(n)} = \sum_{j=1}^{M-1} \frac{a_j^{(n)}}{s - p_j} + a_M^{(n)} = a_M^{(n)} \frac{\prod_{i=1}^{M-1} \left(s - z_i^{(n)}\right)}{\prod_{j=1}^{M-1} (s - p_j)}. \tag{1.13}$$

Due to the structure of equation (1.11), poles of the transfer function under norm in (1.11) are the zeroes of (1.13). In this way the iterative process uses a new set of poles $\{z_i\}$ at each iteration, so improving the approximation. This scheme is known as "pole-relocation".
Authors in [4] gives some practical hints for choosing the starting poles $\{p_i\}$, in order to obtain a good convergence of the iterative process.
A further improvement of numerical conditioning of VF can be achieved using an orthonormal set of basis functions as shown by Deschrijver and Dhaene (2005) [11] [12] [13] [14].

1.3 The Rational Function Approximation algorithm

In this section we show how the identification of a rational approximation in the form:

$$f(s) = \frac{r_0 + r_1 s + r_2 s^2 + \ldots + r_N s^N}{a_0 + a_1 s + a_2 s^2 + \ldots + a_N s^N} = \frac{N(s)}{D(s)}, \tag{1.14}$$

may be pursued by solving two overdetermined linear systems. This method is known as Rational Function Approximation (RFA) (Elzinga et al 2000 [15] [16], Gao et al 2005 [8]).
The identification is performed in the frequency domain, so we set $s = j\omega$. In order to obtain purely real coefficients $\{r_i\}$ and $\{a_i\}$, only the real part of the frequency response is used in the approximation. In fact, the real part of a system response $f(s)$ is an even function and its poles are those of both functions $f(s)$ and $f(-s)$. Since the system is known to be stable, those poles belonging to $f(s)$ lie in the left half of the complex plane.
The real part of the original function is fitted with the real rational polynomial function of the squared variable:

$$Re\{f(j\omega)\} = \frac{\tilde{r}_0 + \tilde{r}_1 \omega^2 + \ldots + \tilde{r}_N \omega^{2N}}{\tilde{a}_0 + \tilde{a}_1 \omega^2 + \ldots + \tilde{a}_N \omega^{2N}}. \tag{1.15}$$

A linear least square problem gives the the denominator of (1.14). The real part of the frequency response at the sampling points is equated to (1.15). The A matrix of the LS problem $Ax \approx b$ is:

$$A = \begin{pmatrix} 1 & \omega_0^2 & \cdots & \omega_0^{2N} & -\omega_0^2 Re(f(j\omega_0)) & -\omega_0^4 Re(f(j\omega_0)) & \cdots & -\omega_0^{2N} Re(f(j\omega_0)) \\ 1 & \omega_1^2 & \cdots & \omega_1^{2N} & -\omega_1^2 Re(f(j\omega_1)) & -\omega_1^4 Re(f(j\omega_1)) & \cdots & -\omega_1^{2N} Re(f(j\omega_1)) \\ \vdots & \vdots & & \vdots & \vdots & \vdots & & \vdots \\ 1 & \omega_k^2 & \cdots & \omega_k^{2N} & -\omega_k^2 Re(f(j\omega_k)) & -\omega_k^4 Re(f(j\omega_k)) & \cdots & -\omega_k^{2N} Re(f(j\omega_k)) \end{pmatrix} \quad (1.16)$$

whereas the trasposed solution vector x^T is:

$$x^T = \begin{pmatrix} \tilde{r}_0 & \tilde{r}_1 & \tilde{r}_2 & \cdots & \tilde{r}_N & \tilde{a}_1 & \tilde{a}_2 & \cdots & \tilde{a}_N \end{pmatrix}, \quad (1.17)$$

and b vector is:

$$b = \begin{pmatrix} Re\{f(j\omega_0)\} \\ Re\{f(j\omega_1)\} \\ \vdots \\ Re\{f(j\omega_k)\} \end{pmatrix}. \quad (1.18)$$

Once the coefficients are obtained by solving (1.16), the roots of the even function will be obtained from:

$$1 + \tilde{a}_1\omega^2 + \tilde{a}_2\omega^4 + \ldots + \tilde{a}_N\omega^{2N} = 0. \quad (1.19)$$

By taking only the stable poles in the left half plane, and rejecting pure imaginary poles, the partial fraction expansion of the transfer function can be formed as:

$$f(j\omega) = k_0 + \sum_{i=1}^{N'} \frac{k_i}{j\omega - p_i} \quad (1.20)$$

where $N' \leq N$ and $N - N'$ are the numbers of rejected pure imaginary poles. The system transfer function will be obtained by solving the residues from (1.20). This is done in the same manner of Vector Fitting algorithm, and will be explained in the next section (residue identification).
Note that (1.16) becomes seriously ill conditioned or even singular for a wide frequency ranges and high order approximation since the entries of the matrix are powers of ω (e.g. Beyene et al 1998 [17]). To alleviate the problem orthogonal polynomials may be used in the approximation since ordinary power series $\{\omega^0, \omega^1, \omega^2, \omega^3, \cdots\}$ have a very large dynamic range (e.g. Beyene 2001 [18]). Despite this possibility, recent literature quite clearly shows that algorithms like RFA have been almost abandoned, whereas VF is more and more used in many different applications.

1.4 The Vector Fitting algorithm

The VF algorithm performs the rational approximation of a tabulated frequency response in the form:

$$f(s) \approx \sum_{m=1}^{N} \frac{c_m}{s - a_m} + d + sh, \tag{1.21}$$

where the coefficients a_m, c_m, d and h are the unknowns of the problem. The function $f(s)$ is approximated in the least square sense.
The algorithm operates in two stages: poles identification and residue identification. Both stages require the solution of a linear least square problem.

Poles identification

In order to solve the poles identification problem, the algorithm requires the specification of a starting pole set $\{\overline{a}_m\}$, which is then iteratively improved.
A unknown scaling function $\sigma(s)$ is introduced. Starting poles are used to approximate both the functions $\sigma(s)f(s)$, and $\sigma(s)$. In this way, we get the couple of equation:

$$\begin{pmatrix} \sigma(s)f(s) \\ \sigma(s) \end{pmatrix} = \begin{pmatrix} \sum_{m=1}^{N} \frac{c_m}{s-\overline{a}_m} + d + sh \\ \sum_{m=1}^{N} \frac{\widetilde{c}_m}{s-\overline{a}_m} + 1 \end{pmatrix} \tag{1.22}$$

By multiplying $f(s)$ by the rational approximation of $\sigma(s)$, we get the equation:

$$\left(\sum_{m=1}^{N} \frac{c_m}{s-\overline{a}_m} + d + sh \right) = \left(\sum_{m=1}^{N} \frac{\widetilde{c}_m}{s-\overline{a}_m} + 1 \right) f(s), \tag{1.23}$$

which can be also written as:

$$\left(\sum_{m=1}^{N} \frac{c_m}{s-\overline{a}_m} + d + sh \right) - \left(\sum_{m=1}^{N} \frac{\widetilde{c}_m}{s-\overline{a}_m} f(s) \right) = f(s). \tag{1.24}$$

Such equation may be written at those several frequencies s_k, where we have samples of the given function $f(s)$ so obtaining:

$$A_k x = b_k, \tag{1.25}$$

where

$$A_k = \left(\frac{1}{s_k-\overline{a}_1} \quad ... \quad \frac{1}{s_k-\overline{a}_N} \quad 1 \quad s_k \quad \frac{-f(s_k)}{s_k-\overline{a}_1} \quad ... \quad \frac{-f(s_k)}{s_k-\overline{a}_N}, \right) \tag{1.26}$$

$$x = \left(c_1 \quad ... \quad c_N \quad d \quad h \quad \widetilde{c}_1 \quad ... \quad \widetilde{c}_N \right)^T \quad , \quad b_k = f(s_k). \tag{1.27}$$

In this way, we get an overdetermined linear system:

$$Ax = b, \tag{1.28}$$

which can be solved in the least square sense.
Now, let us writing the couple of functions $f(s)$ and $\sigma(s)f(s)$ as ratio of two polynomials:

$$\sigma(s)f(s) = h\frac{\prod_{m=1}^{N+1}(s-z_m)}{\prod_{m=1}^{N}(s-\overline{a}_m)} \quad , \quad \sigma(s) = \frac{\prod_{m=1}^{N}(s-\widetilde{z}_m)}{\prod_{m=1}^{N}(s-\overline{a}_m)}, \tag{1.29}$$

it results $f(s)$:

$$f(s) = \frac{\sigma(s)f(s)}{\sigma(s)} = h\frac{\prod_{m=1}^{N+1}(s-z_m)}{\prod_{m=1}^{N}(s-\widetilde{z}_m)}. \tag{1.30}$$

Last equation indicates that poles of $f(s)$ are the zeroes of $\sigma(s)$. Original starting poles $\overline{a}_m$ disappear, since they are the same for both functions $\sigma(s)$ e $\sigma(s)f(s)$. New poles of $f(s)$ become the zeroes of $\sigma(s)$. They can be determined by calculating the eigenvalues of the matrix:

$$H = A - b\widetilde{c}^T, \tag{1.31}$$

where A is a diagonal matrix holding the previous pole set (at first iteration, they are $\overline{a}_m$), whereas b is a column vector of 1 and $\widetilde{c}^T$ is a row vector holding the residues of $\sigma(s)$.

Residues identification

This stage takes the poles as previously determined in the poles identification stage, and find out the residues of :

$$f(s) \approx \left(\sum_{m=1}^{N} \frac{c_m}{s-\overline{a}_m} + d + sh \right). \tag{1.32}$$

Also this problem involves the solution of an overdetermined linear system in the least square sense:

$$Ax = b \tag{1.33}$$

where vector x holds the unknown coefficients c_m, d and h, whereas the matrix A is made of row:

$$A_k = \left(\frac{1}{s_k-\overline{a}_1} \quad ... \quad \frac{1}{s_k-\overline{a}_N} \quad 1 \quad s_k \right). \tag{1.34}$$

The vector fitting algorithm has been shown on a scalar function, but it may be easily formulated on a matrix of frequency responses. This possibility gives the name of the algorithm.

The accuracy of the end result and/or the possibility of a fast convergence are related to the choice of the initial pole set.
A real pole set (either linearly or logarithmically spaced) may be successfully used when approximating smooth frequency responses. A response with resonance peaks usually requires complex conjugate pairs of poles. Details on this are given in [4].

1.5 The fitting of a magnitude frequency response

In this section we will address the problem of the rational approximation of a magnitude frequency response, so meaning that the phase angle of the given response is not exploited in the fitting process. This situation arises either when only magnitude responses are available from measurements (e.g. Zhang et al 2002 [19]) or when the whole modeling process is specifically designed to ignore the information provided by phase angle. A meaningful example of this will be given in chapter 3, and is related to the identification of the propagation function of a transmission line.

1.5.1 Asymptotic fitting of a magnitude frequency response

Bode (1945) introduced the asymptotic fitting of magnitude functions [20]. Basically, it allocates poles and zeroes by tracking the original function as function of frequency. A new pole/zero is allocated whenever the asymptote of the fitting function deviates from the original function by more than a predefined tolerance. That way, the fitting function freely adapts itself to the shape of the original function. This implies that the order of the approximation is not established "a-priori" but results from the required accuracy specified as input for the fitting routine. The procedure was designed assuming real poles and zeroes located in the left half-plane. Thus, the rational function belongs to the class of minimum phase shift functions.
This approach was used applied to transmission line modelling by J. Marti (1982) [21].

1.5.2 Magnitude fitting via Symmetric Vector Fitting

We have already seen that VF requires knowledge about the both magnitude and phase of the function to be identified. On the other hand, since it is a very accurate and robust algorithm, a magnitude fitting procedure exploiting its pole relocation scheme would be desirable. Such formulation have been developed by De Tommasi and Gustavsen (2006) and is presented in [22]. In the following we describe it in detail.
A rational minimum phase shift function $g(s)$, with N poles and N zeroes, all

located in the left hand side of the complex plane, has a magnitude square $|g(s)|^2$ with $2N$ poles and $2N$ zeroes, which are the N poles and N zeroes of $g(s)$ and their symmetrical counterparts in the right half plane. Note that $|g(s)|^2$ has zero phase angle, being a real function.

$$|f|^2 \cong k\frac{\prod_{m=1}^{N}\left[(s-z_m)(s+z_m)\right]}{\prod_{m=1}^{N}\left[(s-p_m)(s+p_m)\right]}; f_{fit} = \sqrt{k}\frac{\prod_{m=1}^{N}(s-z_m)}{\prod_{m=1}^{N}(s-p_m)} \tag{1.35}$$

This suggests that, once a magnitude square response $|f(s)|^2$ has been fitted (1.35), discarding zeros and poles having positive real part gives a minimum phase shift function $f_{fit}(s)$ whose magnitude fits the magnitude of $f(s)$ in the least squares (LS) sense. In (1.35), we assume both $Re\{z_m\} < 0$ and $Re\{p_m\} < 0$. The standard VF algorithm is suitable for fitting the magnitude square response provided that it gives a rational expansion with symmetrical poles and residues, which implies zero phase angle.

$$|f|^2 \cong \sum_{m=1}^{N} r_m \left(\frac{1}{s-p_m} - \frac{1}{s+p_m}\right) + d \tag{1.36}$$

Thus, the desired rational approximation is on the form (1.36).
In practice, one cannot obtain poles and residues that are perfectly symmetrical with respect to the imaginary axis, since this has not been analytically enforced. Therefore, more robustness and accuracy can be achieved by enforcing the required symmetry with a proper choice of basis functions for the pole identification step of the VF algorithm itself. We refer to such a reformulation of the VF algorithm as Symmetric Vector Fitting (SVF). It is worth underlining that this approach is able to improve also the identification of a response from its real part.
Let us consider the pole identification problem referred to magnitude square functions:

$$(|f|^2\,\sigma^2)_{fit} - |f|^2\,\sigma^2_{fit} \approx 0, \tag{1.37}$$

where

$$(|f|^2\,\sigma^2)_{fit}(s) = \sum_{m=1}^{N} c_m \left(\frac{1}{s-q_m} - \frac{1}{s+q_m}\right) + d, \tag{1.38}$$

$$\sigma^2_{fit}(s) = \sum_{m=1}^{N} \overline{c}_m \left(\frac{1}{s-q_m} - \frac{1}{s+q_m}\right) + \overline{d}, \tag{1.39}$$

and $\{q_m\}$ are the starting poles.
Now, let us write the (1.37) in the form $Ax \approx b$, which is needed for the solution

of the LS problem. Let us denote the sums of simple fractions in the concise form:

$$g_{k,m} = \frac{1}{s_k - q_m} - \frac{1}{s_k + q_m}, \tag{1.40}$$

when q_m is a real pole, and

$$g_{k,m} = \frac{1}{s_k - q_m} - \frac{1}{s_k + q_m} + \frac{1}{s_k - q_m^*} - \frac{1}{s_k + q_m^*} \tag{1.41}$$

$$g_{k,m+1} = \frac{j}{s_k - q_m} - \frac{j}{s_k + q_m} - \frac{j}{s_k - q_m^*} + \frac{j}{s_k + q_m^*} \tag{1.42}$$

when $\{q_m, q_{m+1}\}$ is a complex conjugate pair. It has to be remarked that (1.40) and (1.41,1.42) are real quantities.
The k^{th} row of A is given by

$$A_k = [\ A_{k,1} \quad A_{k,2}\ ], \tag{1.43}$$

where

$$A_{k,1} = [\ g_{k,1} \quad \ldots \quad g_{k,N} \quad 1], \tag{1.44}$$

$$A_{k,2} = -|f(s_k)|^2 \cdot [\ g_{k,1} \quad \ldots \quad g_{k,N} \quad 1\ ]. \tag{1.45}$$

The solution vector x, in the case of real poles is

$$x = \left(\ c_1 \quad \ldots \quad c_N \quad d \quad \bar{c}_1 \quad \ldots \quad \bar{c}_N \quad \bar{d}\ \right)^T. \tag{1.46}$$

The right side b is

$$b = \left(\ 0 \quad \ldots \quad 0\ \right)^T. \tag{1.47}$$

For complex conjugate pairs, the (1.41,1.42) enforce that correspondent residues will come out in complex conjugate pairs too. Being $c_m = c' + jc''$ and $c_{m+1} = c' - jc''$, the correspondent elements into x will be c' and c''.
Note that we must avoid the trivial null solution of LS problem $Ax \approx 0$. In order to do this, the additional row:

$$\sum_{k=1}^{N_s} \left(\sum_{m=1}^{N} g_{k,m}\bar{c}_m + \bar{d} \right) = N_s, \tag{1.48}$$

is added to (1.37) [10], giving the non-zero vector

$$b = \left(\ 0 \quad \ldots \quad 0 \quad N_s\ \right)^T. \tag{1.49}$$

The solution of the LS problem must give a positive d term, since the identified magnitude square function cannot assume negative values. This may be obtained by solving a constrained LS problem. However, we verified that even avoiding such a constrained formulation, a positive d can be easily obtained by selecting

a different order of approximation.
After the LS problem has been solved, the zeroes of $\sigma^2_{fit}(s)$ must be calculated, writing the (1.39) on the form

$$\sigma^2_{fit}(s) = \sum_{m=1}^{N} \left(\frac{2\overline{c}_m q_m}{s^2 - q_m^2} \right) + \overline{d} = \overline{d} \frac{\prod_{m=1}^{N} (s^2 - \bar{z}_m^2)}{\prod_{m=1}^{N} (s^2 - q_m^2)}. \tag{1.50}$$

The quantities $\{\bar{z}_m^2\}$ are computed as explained in the section (1.4); their square roots are the needed zeros $\{\bar{z}_m\}$ to be assigned as new poles $\{p_m\}$ in (1.36).
Since a single imaginary pole cannot appear in $f_{fit}(s)$ (1.35), if any negative $\{\bar{z}_m^2\}$ occur during the VF iterations, their sign have to be changed before extracting the square root.

1.5.3 Discussion

The algorithm described in section (1.5.2) presents two recognized drawbacks.
First one concerns the analytic form of the rational function (1.36). In fact, it is not positive definite as a magnitude square function should be. Experience shows that it may take negative values when functions vanishing for $s \to \infty$ are fitted. Such negative values can be removed by increasing the fitting accuracy around those frequencies where negative values are taken, either by increasing the fitting order or by increasing the local weighting for the LS problem. We prefer the second option in order to avoid an unnecessary high order. This approach will be used in chapter 3, for the fitting of propagation functions.
Second drawback concerns the possibility of some negative $\{\bar{z}_m^2\}$ appearing during the iterations. By changing their sign before calculating $\{\bar{z}_m\}$, a perturbation is introduced. For this reason, the convergence may fail when fitting very noisy responses.

1.5.4 Test cases

In this section some test cases will be analyzed, in order to show the validity of the proposed magnitude fitting algorithm.

A power distribution system

First test case refers to a calculated terminal admittance matrix $Y(s)$ of the power distribution system shown in fig. (1.1). It has two 3-phase buses as terminals (A, B). The 6×6 admittance matrix Y with respect to these terminals has been evaluated in the frequency interval [10 Hz,100 kHz].
Such example is included in the package `vfit2`, and is described in its user guide (`ex4.m`). Here we pursue the identification of the matrix Y element by element.

Figure (1.2) shows the identification of the magnitude for the component Y_{12}, whereas fig. (1.3) shows the minimum phase angle of the identified function compared to the reference, which is not a minimum phase shift. The number of poles is $N = 36$.

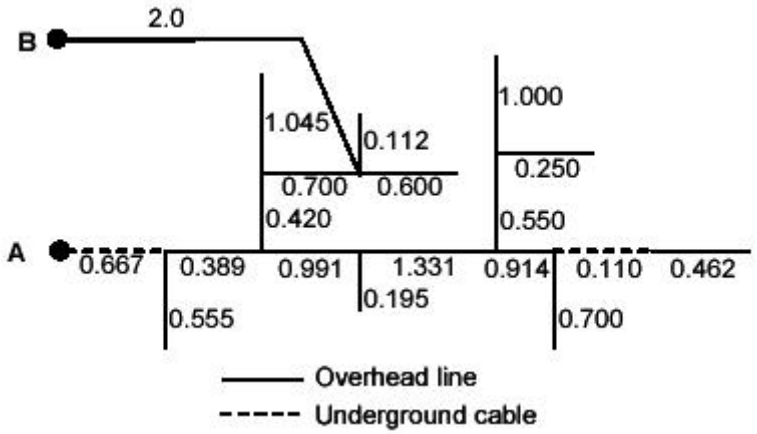

Figure 1.1: Magnitude Fitting, test case 1 : A power distribution system

A rectifier transformer

Second test case refers to a measured admittance matrix $Y(s)$ of a 3-winding rectifier transformer (Gustavsen 2003 [23]). The admittance matrix was measured in the frequency domain using a network analyzer and a dedicated measurement setup. Subsequent its approximation with rational functions gives an EMTP-type compatible model suitable for transient studies. In [23], the rational approximation was used for the calculation of internal voltages in a winding. Here, differently from [23], we assume that only the magnitude is available from measurements.
Figure (1.4) shows the identification of the magnitude for the component Y_{11}, whereas fig. (1.5) shows the minimum phase angle of the identified function compared to the reference. The number of poles is $N = 60$. Note that:

- the identification process can only guarantee that the magnitude of the minimum phase shift rational function fits the magnitude of the reference function in the limited band $[f_1, f_2]$ where the reference function is assigned;

- there does not exist a unique minimum phase angle associated to a magnitude function given on a limited frequency band $[f_1, f_2]$, since the shape of the magnitude function in the whole frequency band $[0, \inf[$ does influence on the phase angle in the band $[f_1, f_2]$. This will be explained in detail in chapter3.

These issues explains the partial disagreement among the two phase angles seen in fig. (1.5), which are both minimum phase shift.

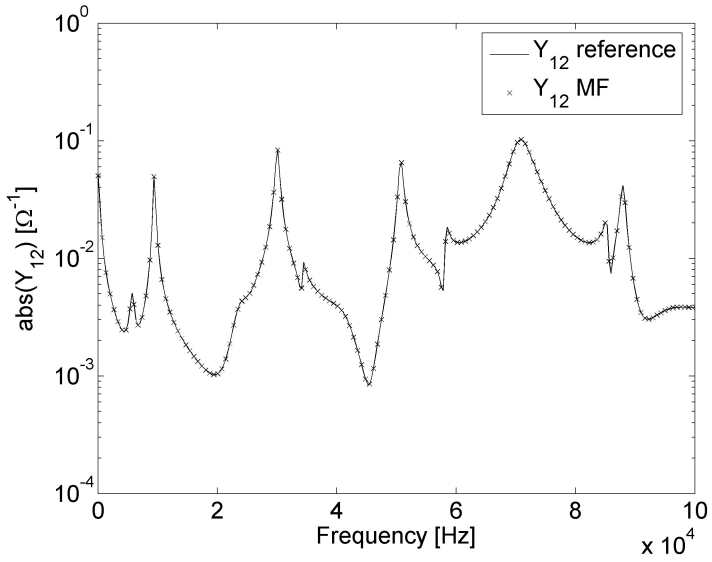

Figure 1.2: Magnitude Fitting, test case 1: Identification of magnitude of Y_{12} (N=36)

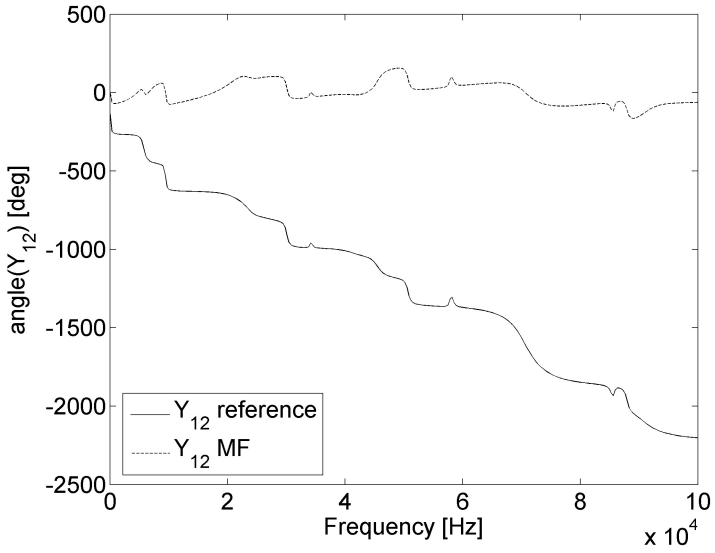

Figure 1.3: Magnitude Fitting, test case 1: Identified minimum phase angle for Y_{12} (N=36) compared to the original

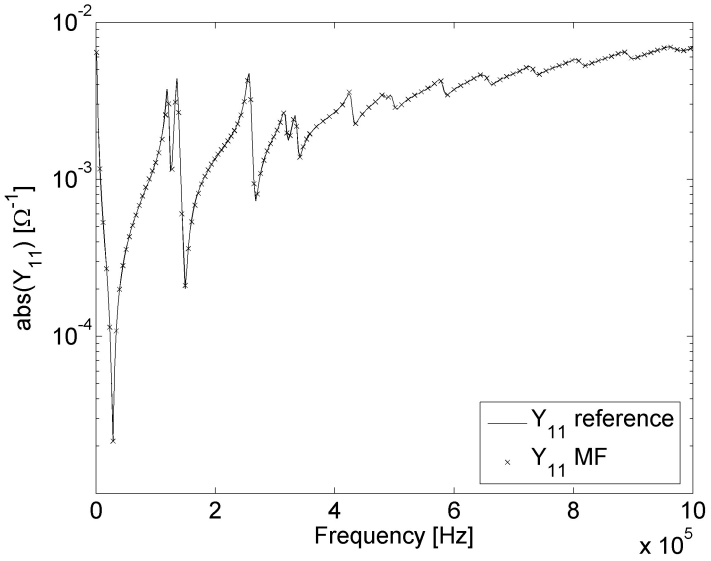

Figure 1.4: Magnitude Fitting, test case 2: Identification of magnitude of Y_{11} (N=60)

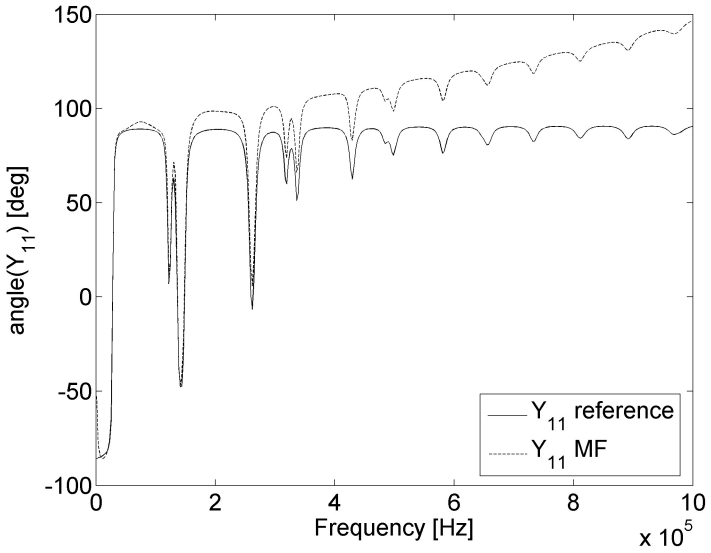

Figure 1.5: Magnitude Fitting, test case 2: Identified minimum phase angle for Y_{11} (N=60)

1.6 Pole repetitions and compact realizations

In this section we consider an identification strategy based on both VF algorithm and a non-linear least square, leading to very accurate approximation and to the

most general state space realization of the transfer function.
State space realizations of transfer functions may be either directly accepted from the time domain simulation environment or converted into a equivalent-circuit network (e.g. Neumayer et al 2002 [24]).
Let us start by considering a minimal state space realization $\{A, B, C, D\}$ of a given transfer function; through a similarity transformation we can obtain the realization having:

$$A = diag\left(\bar{p}_1, \cdots, \bar{p}_{N^*}\right). \tag{1.51}$$

The following relation holds:

$$C\left(sI - A\right)^{-1} B + D = \sum_{i=1}^{N*} \frac{K_i}{s - \bar{p}_i} + D. \tag{1.52}$$

It results $K_i = c_i b_i^T$, where c_i is the i^{th} column of C, and b_i^T is the i^{th} row of B. Note that $rank\left(K_i\right) = 1$, being K_i the product of a column by a row.
On the other hand, the most general form of a rational approximation of a $m \times m$ transfer matrix $H(s)$ is:

$$\tilde{H}(s) = \sum_{i=1}^{N} \frac{R_i}{s - p_i} + D \tag{1.53}$$

where $rank(R_i) = m, \quad \forall i$.
By performing the following singular value decompositions:

$$R_i = U_i \cdot S_i \cdot V_i^T \tag{1.54}$$

where U_i and V_i are unitary matrices, and S_i is a diagonal matrix containing the singular values $\{\sigma_i\}$ in descending order:

$$S_i = diag(\sigma_1, \ldots, \sigma_m), \tag{1.55}$$

each residue R_i can be separated in the sum of matrices $\{R_{ij}\}_{j=1\ldots m}$ having $rank(R_{ij}) = 1$. Each of R_{ij} is obtained by including in the decomposition only a singular value at one time, and replacing the others with zero:

$$S_{ij} \equiv diag(0, \ldots, \sigma_j, \ldots, 0), \tag{1.56}$$

$$R_{ij} \equiv U_i S_{ij} V_i^T, \tag{1.57}$$

$$R_i = U_i \cdot \left(\sum_{j=1}^{m} S_{ij}\right) \cdot V_i^T = \sum_{j=1}^{m} U_i \cdot S_{ij} \cdot V_i^T = \sum_{j=1}^{m} R_{ij} \tag{1.58}$$

Now, we can rewrite the function $\tilde{H}(s)$ in the following form:

$$\tilde{H}(s) = \sum_{i=1}^{N} \sum_{j=1}^{m} \frac{R_{ij}}{s - p_i} + D = \sum_{n=1}^{N^*=mN} \frac{K_i}{s - a_i} + D, \tag{1.59}$$

which shows that the effective equivalent circuit order of (1.53) (order of a minimal state space realization) is $N^* = mN$ and that each pole p_i will appear in the A matrix (1.51) with m repetitions. Since normally N^* is fixed as degree of complexity of the equivalent dynamic network, the case of $rank(R_i) = r > 1$ have to be avoided in the identification process, because it corresponds to constrain r elements on the diagonal of (1.51) to be equal, so limiting the accuracy of the identification at a fixed order.
Unfortunately, the constraint $rank\,(R_i) = 1 \quad \forall i$ cannot be explicitly enforced as long as the identification process is based on linear procedures, such as the MBPE algorithm [24], the Subspace System Identification algorithm (e.g. Grivet-Talocia et al 2002 [25]), or the VF algorithm [4] [26]. In fact, in the general case the use of any of these methods provides residues $\{R_i\}$ having full rank.
In order to get a state space realization having the general form (no pole repetitions in A matrix and B full), a post-processing technique based on a SVD and a NLLS algorithm has been proposed (Gustavsen 2004 [27]). This procedure eliminates the pole repetitions in the matrix A through the rank reduction of residue matrices $\{R_i\}$. By performing the singular value decomposition (1.54), it can be verified that, in many practical cases, first singular values in (1.55 are much larger than the rest, thus permitting the smallest to be set equal to zero. A tolerance ε is fixed in order to decide which is the smallest singular value σ_r to be retained:

$$\frac{\sigma_r}{\sigma_1} < \varepsilon \tag{1.60}$$

This is related to the needed accuracy of the final approximation: if it is not met by using a certain tolerance ε, it is necessary to reduce the value of ε. When only the first r singular values are retained, the rank of the corresponding matrix R_i becomes r, so reducing the number of repetitions of the pole P_i in the matrix A from m to r. This is called "compacting". It is also evident that this approximation of the residue matrices produces an error in the compacted state space realization. The error can be reduced by subjecting the compacted state space realization to an error minimization procedure, which is based on a nonlinear least square algorithm (either Gauss-Newton or Levenberg-Marquardt). The main drawback of the described approach is the lack of an analytical relation between the parameter ε of (1.60) and the target accuracy of the rational approximation. This implies that if ε needs to be adjusted, the procedure of compacting and nonlinear optimization needs to run again. For this reason, we proposed a new procedure overcoming these limitations. It still uses the VF algorithm to obtain a very good initial guess to be used by NLLS for finding a more accurate state space realization of the same order with no pole repetitions. The goal of eliminating pole repetitions in the matrix A is achieved avoiding the compacting procedure (discarding of singular values).
The procedure operates as follow: the vector fitting algorithm is launched using

N poles; then, so determined rational approximation is used as starting guess for the non-linear identification. The order of the state space realization N^* does not change after applying the non-linear procedure.
The pole-residue form with rank-1 residues enables the immediate derivation of an equivalent-circuit network (e.g. Mangold and Russer 1999 [28]). This approach represents the straightforward generalization of a general synthesis procedure for any constant m-port admittance (Cauer 1932 [29]). Evidently, such a synthesis can be also performed before that pole repetitions have been eliminated through the application of the NLLS algorithm, but this would give a less accurate result.
In the following, we show the cost function to be minimized when identifying a symmetric matrix 2×2 of smooth responses (only real poles are used in the identification), assuming unitary weighting (i.e. $\gamma_{pqk} = 1, \forall p, q, k$ in eq. (1.9)):

$$\chi_{2\times 2}(\{r_{1i}\},\{r_{2i}\},\{p_i\},D) = \sum_{k=1}^{N_s} \left\| H(s_k) - \sum_{i=1}^{N} \frac{\begin{pmatrix} r_{1i} & r_{1i}r_{2i} \\ r_{1i}r_{2i} & r_{1i}r_{2i}^2 \end{pmatrix}}{s_k - p_i} - D \right\|_F^2 . \tag{1.61}$$

1.6.1 Computational cost of the time domain simulations

Let us move to some considerations on the computational cost of the time domain simulations.
Such a cost is evaluated as the number of elementary numerical operations (addition, multiplication) for each time step and depends on the implementation of the time domain model.
Gustavsen in [27] compared the computational efficiency of the compacted state space realization with the original one (having pole repetitions), referring to the implementation supported by the EMTP simulator, which handles the state space realizations. He found that the compacted realization is more efficient of a factor $m/2$. However, it has to be remarked that the whole procedure for the elimination of pole repetitions (compacting + NLLS) leads to a less accurate approximation than the original (the order is lower). Instead, our procedure does not reduce the order of the state space realization (it does not include any compacting), but improves the accuracy at the same order through the NLLS identification.
A different time domain scheme was considered by de Magistris and De Tommasi (2005) in [30]. It leads to a slightly different evaluation of the computational cost. They assumed that the recursive convolution is performed by exploiting the tranfer function, so avoiding the derivation of a state space realization. Since residues R_i are $m \times m$ matrices having $rank\{R_i\} = 1$, for each pole p_i only m convolution between inputs and corresponding elements of a single row of R_i must be calculated; the contributions given by the others $m - 1$ rows is simply

computed by performing $m-1$ multiplications. This indicates that the additional burden in time domain simulation added by the refinement process concerns only $m-1$ multiplications per matrix residue, since the total number of recursive convolution to be performed does not increase. In order to compare the efficiency of the pure VF approach and the combined procedure, we assume as a measure of computational cost the number of multiplications to be performed per time step. By exploiting a routine which performs the recursive convolution with a single pole as in [31], the cost is three multiplication per time step. The pure VF approach gives the computational cost:

$$C_{VF}(N) = 3 \cdot m^2 \cdot N, \tag{1.62}$$

where N is the number of poles. Instead, our combined procedure gives:

$$C_{VF+NLLS}(N) = (4 \cdot m^2 - m) \cdot N, \tag{1.63}$$

According to this time-domain implementation, the VF+NLLS gives a higher cost than pure VF. However, in several cases it may be still more advantageous a VF+NLLS identification than a pure VF identification with $N' > N$.
In addition, here we give a practical consideration on time domain implementation based on the state space realizations. In such a case, the B matrix becomes full after the application of the NLLS, whereas that one originally provided by VF algorithm is sparse [26]. In principle, this would increase the computational cost of the numerical integration, since when the matrix is known to be sparse, some calculations can be avoided [27]. But if we perform integration through highly efficient built-in functions of the simulation environment, they cannot take into account the sparsity of some matrices of the state space realization, being written for the general case. This means that the simulation will not cost more after having run the NLLS algorithm. On the other hand, if the accuracy were improved just using the VF algorithm alone with an increased number of poles $N' > N$, the corresponding time domain simulation would cost more, since the size of A matrix would have been increased.

1.6.2 Test cases

As application of the described procedure we consider the identification of two frequency responses analyzed in [30]. They represents the regular parts of a characteristic admittance/impedance of an RLGC transmission line, whose definitions will be given in chapter 3.
In order to study the accuracy, we introduce the rms-error:

$$\sigma(i,j) = \sqrt{\sum_{k=1}^{N} \left| H_{ij}(j\omega_k) - \tilde{H}_{ij}(j\omega_k) \right|} \tag{1.64}$$

where $H(s)$ is the given transfer matrix and $\tilde{H}(s)$ the identified one.
Figure (4.19) shows the identification of a Y_{cr} component with the proposed procedure, whereas fig. (1.7) the identification of a Z_{cr} of a different dataset. In both cases, unitary weights have been used, i.e. $\gamma_{pqk} = 1, \forall p, q, k$ in eq. (1.9). The two example show that a sensible fitting accuracy improvement is achievable by running the NLLS procedure after the VF algorithm.

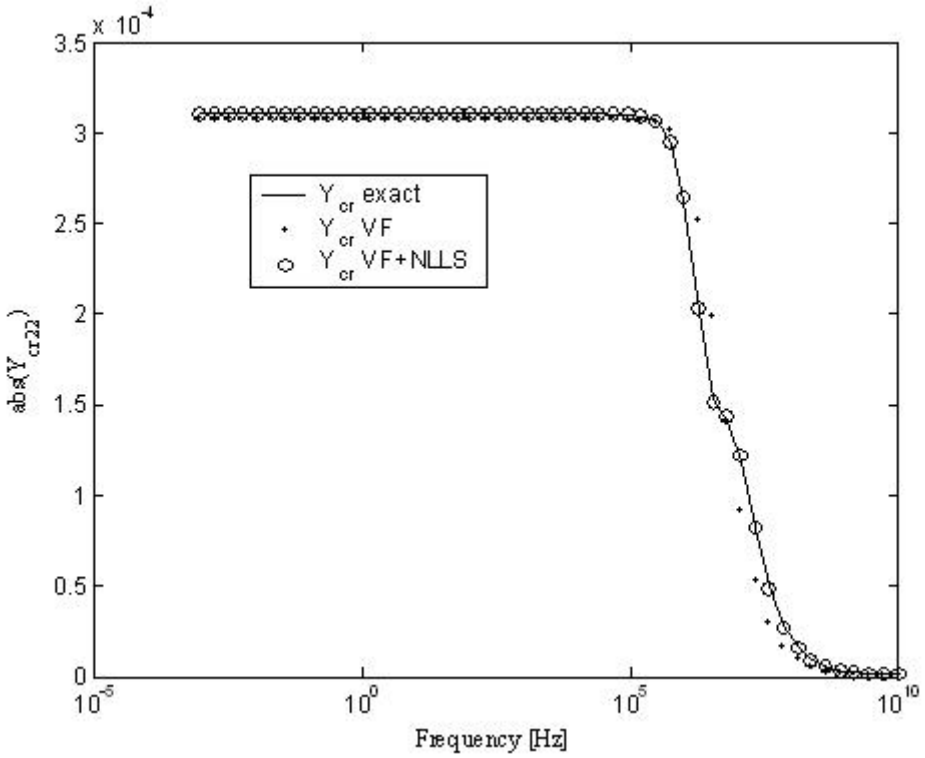

Figure 1.6: Identification with VF compared to VF+NLLS : Y_{cr22} component of a four conductor transmission line

Table 1.1: Identification with VF compared to VF+NLLS : rms errors on components of Y_{cr}

rms error	VF	VF + NLLS
σ_{11}	7.60e-6	6.47e-6
σ_{12}	3.13e-6	2.32e-6
σ_{13}	1.46e-5	6.21e-6
σ_{22}	1.78e-5	1.46e-6
σ_{23}	3.13e-6	2.32e-6
σ_{33}	7.60e-6	6.47e-6

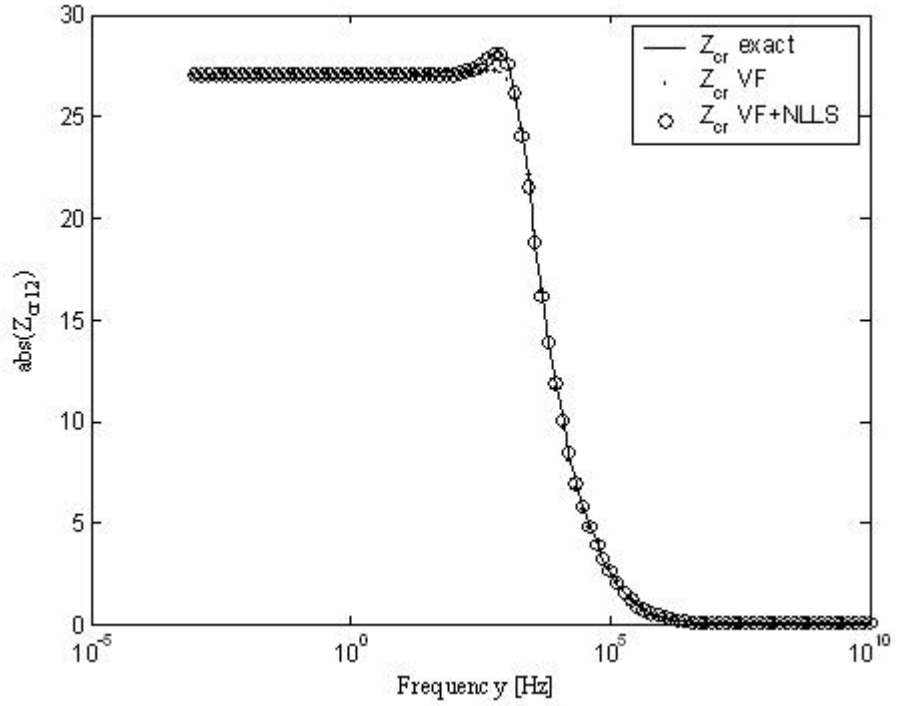

Figure 1.7: Identification with VF compared to VF+NLLS : Z_{cr12} component of a three conductor transmission line

Table 1.2: Identification with VF compared to VF+NLLS: rms errors on components of Z_{cr}

rms error	VF	VF + NLLS
σ_{11}	5.80e-1	5.72e-1
σ_{12}	2.92e-1	2.91e-2
σ_{22}	5.80e-1	5.71e-1

Chapter 2

Black box modelling

2.1 Introduction

There are a large number of reduced order models of electric/electronic systems which needs to be identified without specific assumptions on the physics of the electromagnetic structure. This is usually referred as "black box" approach.
Black box frequency domain identification has been applied with success to a variety of electric/electronic systems. In particular in the area of power systems, high voltage transformers (Gustavsen 2004 [32] [33]) are quite often efficiently modeled by lumped circuit equivalents by means of frequency domain identification in view of simulating the whole network under lightning conditions, which need high frequency models. On the other hand such approach is also present in the reduced modeling of high-speed interconnects like vias and high speed interconnects operating in non-TEM conditions (Chiariello et al 2005 [34]).
In all cases measured/simulated multi-port descriptions, in the form of transfer matrices as function of frequency, are supposed to be known in the range of interest, which often spans from 0 to 10-50 MHz for the power systems and from 0 to 10-20 GHz for electronic interconnects. Scattering representation S is surely the most general since it is never singular. Nevertheless in many cases more familiar Y or Z representations are successfully used.
Note that structures we consider are passive multiports, i.e. they cannot generate energy. The interconnection of passive multiports is guaranteed to be stable, whereas stable but nonpassive systems may become unstable depending on the termination networks. This means that identified reduced order models have to be not only accurate but also passive as the structures they represent.
In this chapter it is assumed that a wide band black box identification of these systems is approached by means of the VF algorithm. In addition, the issue of passivity enforcement on the identified reduced order models is presented. The

most known algorithms for passivity enforcement are rewieved to analyze and compare their features.
Then, a test case of practical importance is fully developed using the VF algorithm and the Hamiltonian perturbation passivity enforcement algorithm.

2.2 Passivity enforcement

Literature has widely shown that issue of passivity enforcement is of primary importance (Gustavsen and Semlyen 2001 [35] [36] [37], Grivet-Talocia 2004 [38], Gao et al 2005 [8]). In fact the identified transfer function of Y, Z or S parameter, may not satisfy the passivity property even when original data do. In such a case, when the identified model is connected to an external network, time domain simulated waveforms may become unstable, exhibiting exponentially growing oscillations. Therefore passivity must be checked and eventually enforced properly.
From a mathematical point of view, passivity property of a multiport circuit is equivalent to the conditions that its transfer matrix $H(s)$ is Positive Real (PR), in case of impedance, admittance or hybrid representation, or Bounded Real (BR), in case of scattering representation (e.g. Anderson and Vongpanitlerd 1973 [39]). When only strictly stable systems with no poles on the imaginary axis are considered, the positive real property becomes:

$$\lambda_i(j\omega) \geq 0 \quad \forall\omega,\ \forall i, \tag{2.1}$$

where λ_i is the i^{th} eigenvalue of the real part of the considered transfer matrix $H(s)$. Condition (2.1) can be directly applied for testing passivity, but requires a frequency sweep, since in principle it has to be checked at any frequency. Most approaches for passivity enforcement are of perturbative kind, involving a post processing step on the identified transfer matrix $H(s)$. They can be given either on the pole-residue form or on a minimal state space realization.
In order to simplify the optimization problem, usually poles are retained as fixed in the passivity enforcement process.

2.2.1 Passivity enforcement by quadratic programming

Gustavsen and Semlyen (2001) introduced a method for passivity enforcement based on the perturbation of pole-residue identified transfer functions through a quadratic programming optimization algorithm.
It assumes that an accurate rational approximation of either admittance matrix $Y(s)$ or impedance $Z(s)$ has been calculated:

$$Y_{fit}(s) = \sum_k \frac{C_k}{s - a_k} + D + sE. \tag{2.2}$$

In such case, it is possible to force any negative eigenvalue of $G_{fit} = Re\{Y_{fit}(s)\}$ to become positive by making only a slight correction to all or some of the parameters $\{C_k\}, \{a_k\}, D$ and E. This allows the linearization of the relation between $eig[Re\{Y(j\omega)\}]$ and the parameters to be corrected.
First, parameters are placed in a single vector x and the columns of Y_{fit} are stacked in a vector y_{fit}. Then (2.2) is linearized so giving an incremental relation such as:

$$\Delta y_{fit} = M\Delta x, \tag{2.3}$$

where details of the calculation of M are given in the appendix of [35]. A linear relation also results between $g_{fit} = Re\{y_{fit}\}$ and Δx being:

$$\Delta g_{fit} = Re(M)\Delta x = P\Delta x, \tag{2.4}$$

where vector g_{fit} stacks columns of G_{fit}. After this, it is necessary to linearize the relation between the eigenvalues λ of $G_{fit} = Re\{Y_{fit}\}$ and the elements of g_{fit} as well:

$$\Delta\lambda = Q\Delta g_{fit}. \tag{2.5}$$

Combining the (2.4) and (2.5) we get:

$$\Delta\lambda = QP\Delta x = R\Delta x. \tag{2.6}$$

The algorithm finds the minimum of the cost function:

$$\chi = \|y(s) - y_{fit}(x,s)\| = \left\|y(s) - \left(y^0_{fit}(x,s) - M\Delta x\right)\right\| \tag{2.7}$$

requiring that eigenvalues λ of G_{fit} are positive. The optimization problem to be solved is the minimization of:

$$\chi = \frac{1}{2}\Delta x^T A^T A\Delta x - A^T b\Delta x, \tag{2.8}$$

subject to

$$-R\Delta x \leq \lambda. \tag{2.9}$$

The method requires a frequency sweep in order to detect violation bands, and enforces the passivity only at a finite set of frequencies. Its effectiveness has been widely shown on power transformer admittances and power transmission line PI-equivalents. A major drawback of such approach is that it can give wrong results when the sampling is not enough accurate.

2.2.2 Passivity enforcement by Hamiltonian matrix perturbation

A different method which detects violations on the whole frequency axis avoiding a frequency sweep was introduced by Grivet-Talocia (2004).
It detects passivity violations by checking the presence of imaginary eigenvalues

of the Hamiltonian matrix of the minimal state space realization of the identified transfer matrix:

$$N_0 = \begin{pmatrix} A - B\left(D + D^T\right)^{-1} C & -B\left(D + D^T\right)^{-1} B^T \\ C^T\left(D + D^T\right)^{-1} C & -A^T + C^T\left(D + D^T\right)^{-1} B^T \end{pmatrix}. \tag{2.10}$$

If this matrix presents any imaginary eigenvalue, the model is not passive; at the corresponding frequencies at least one of the eigenvalues of $Re\{H(j\omega)\}$ changes in sign.
Furthermore, analyzing imaginary eigenvalues of N_0 and their eigenvectors, the set of frequency interval $\{(\omega_i, \omega_{i+1})\}$ where violations occur, can be determined. Then, an iterative scheme giving first order perturbations to the elements of C matrix, is used for correcting the model. In particular, the location of Hamiltonian imaginary eigenvalues are related to the elements of C matrix through a first order expansion. This suggests an iterative scheme to apply first order perturbations for correcting the model. The algorithm operates as follows:

1. compute the set Λ of imaginary eigenvalues of Hamiltonian matrix N_0
2. while $\Lambda \neq \{\phi\}$
3. determine the violation bandwidhts $\{\omega_{i-1}, \omega_i\}$
4. extimate maximum singular value γ_{max} in each violation bandwidht
5. perturb the imaginary eigenvalues and compute correction matrix Δ
6. $C = C + \Delta$
7. compute the set Λ of imaginary eigenvalues of Hamiltonian matrix N_0
8. end while

The described method detects violation on the whole frequency axis and does not need a frequency sweep. Its effectiveness has been demonstrated on interconnects and electronic packaging data sets [38].

2.2.3 Passivity enforcement by convex optimization

A more general approach is introduced by Coelho et al. (2004) [40], being no longer a perturbative one. In such formulation PR constraints are given in the form of linear matrix inequalities (LMIs) on a minimal state space realization (A, B, C, D). If, and only if, there exists a $K = K^T$ such that the following LMIs are satisfied:

$$\begin{bmatrix} -A^T K - KA & -KB + C^T \\ -B^T K + C & D + D^T \end{bmatrix} \geq 0, \quad K \geq 0 \tag{2.11}$$

the transfer function $H(s) = C(sI - A)^{-1}B + D$ is PR. The term E proportional to s, can be included in the transfer function ($H(s) = C(sI - A)^{-1}B + D + sE$); it must satisfy $E = E^T$ and $E \geq 0$.
Note that positive real constraints are convex in both C, D and E [6]. This suggests an algorithm that exploits the knowledge of the poles of a previously determined model (not necessarily positive real), whereas C, D and E matrices are calculated solving a convex optimization problem. In this way, the passivity constraint is directly taken into account in a new identification process which fits in the least square sense the given data set.

2.2.4 Discussion

Although a complete comparison among the approaches involving different kinds of data sets is still not available, some general comments on each of the considered algorithm can be given.
Approach introduced by Gustavsen and Semlyen (2001) gives an optimal flexibility to implement several strategies to perform the needed corrections, since the location and the number of samples for solving the constraint problem can be adapted to the specific case. It is limited only to admittance-impedance representations.
Approach introduced by Grivet-Talocia (2004) is suitable for any representation for the transfer function (including scattering), and exactly enforces passivity at any frequency.
Approach introduced by Coelho et al (2004) is by far the more general and robust, but is quite difficult to implement and with high computational cost. Therefore it seems to be practically limited to low order models.

2.3 A test case: modelling of unshielded twisted cables

In this section we show the black box modeling approach of unshielded twisted pairs (UTPs). They nowadays finds a great concern in high speed computer networking systems, because of their capability to reduce the EMI effects induced by external fields, and the crosstalk produced by parallel wires.
UTPs susceptibility and crosstalk have been extensively examined in the past adopting analytical and numerical techniques (Paul and McKnight 1979, Chamberlin et al 1995 [41], Schutt-Aine 2001 [42], Caniggia et al 2004 [43]), mainly using a transmission line (TL) modelling of UTPs. However, at high frequencies the TL model is not expected to be valid any longer, due to radiation, dispersion, etc. Full-wave numerical methods are in principle suitable to model all the phenomena occurring in UTPs. However, they require significant computational burden, hence making very hard the simulation of entire UTPs interconnects running for several meters. To overcome this problem, Caniggia et al (2006) [44]

proposed to use a threedimensional full wave surface integral formulation (Miano and Villone 2005 [45]) to predict the terminal behavior of only a limited length of the UTPs line. Then, a circuit extraction technique is applied to derive an equivalent circuit model suitable for the analysis by any commercial circuit simulator. Cascading several such equivalent circuits a representation of UTPs interconnections of any length can be obtained.
A computer code (named SURFCODE) based on the mentioned integral formulation [45] has been used to derive the admittance matrix of two twist pitches (around 3 cm) of an UTP, see fig. (2.1).
We here derive a more general lumped representation, i.e. a state space realization, on which the passivity is also enforced. Differently from [44], after the identification of the reduced order model with VF algorithm, the presence of some passivity violations is checked. Then, they are corrected through the procedure based on Hamiltonian perturbation [38] as implemented in the IdEM (Identification of Electrical Macromodels) computer code, available at:
`http://www.emc.polito.it/software/IdEM/doc/idem_readme.htm`.
Figures (2.2) and (2.3) shows the identification of the term $Y_{11} = Y_{22}$, whereas fig. (2.4) and (2.5) the term $Y_{12} = Y_{21}$. Both couple of figures refers to the final result, after the passivity enforcement process. Figures (2.6) and (2.7) shows how the passivity enforcement process is able to correct violations.

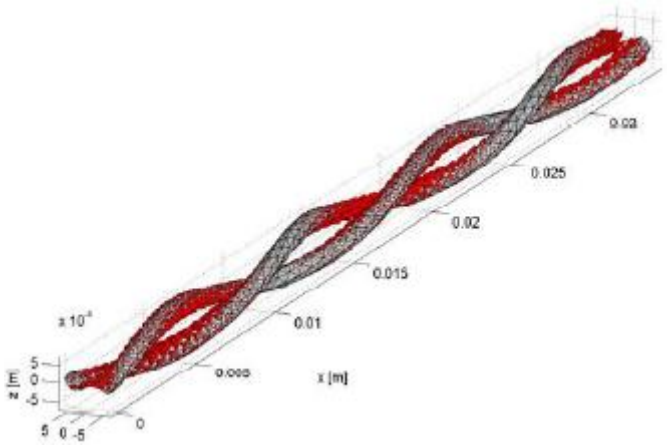

Figure 2.1: Twisted cable : reference geometry.

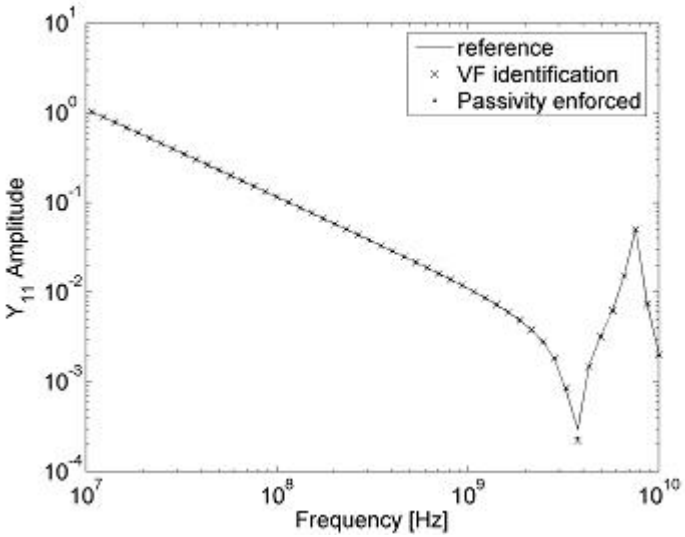

Figure 2.2: Twisted cable : identification of the magnitude of Y_{11}.

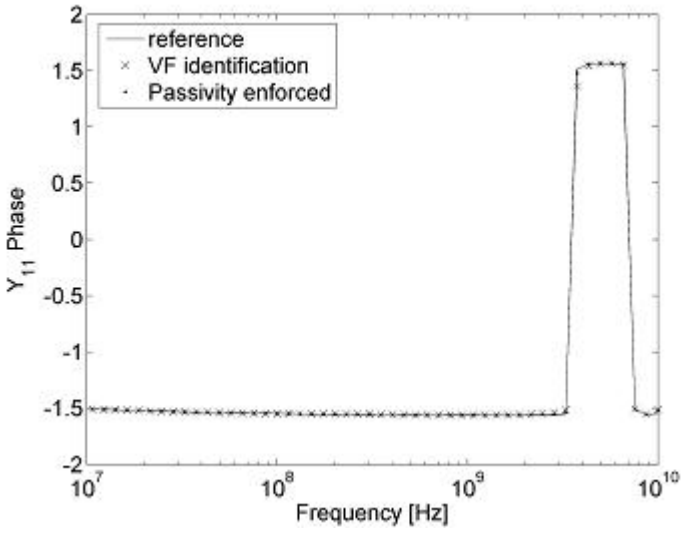

Figure 2.3: Twisted cable : identification of the phase angle of Y_{11}.

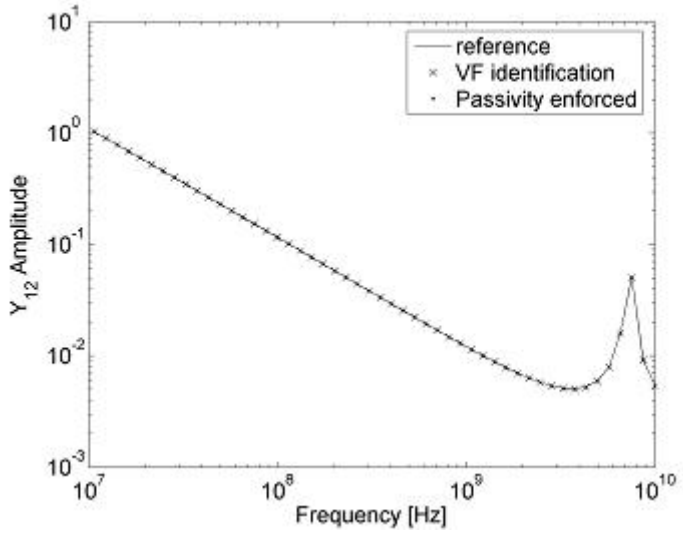

Figure 2.4: Twisted cable : identification of the magnitude of Y_{12}.

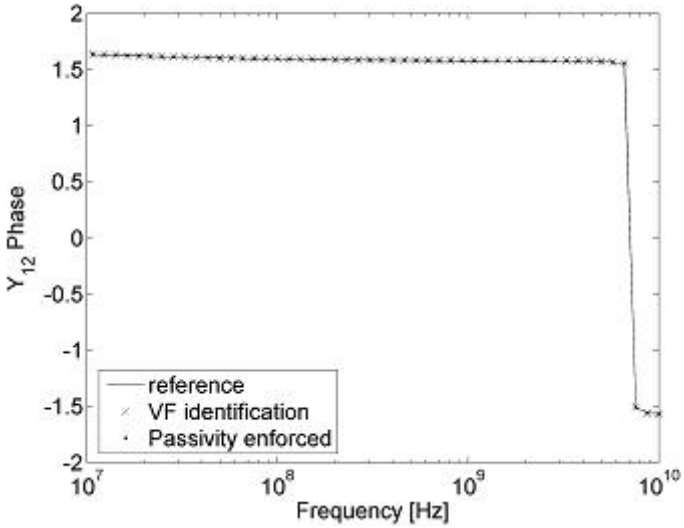

Figure 2.5: Twisted cable : identification of the phase angle of Y_{12}.

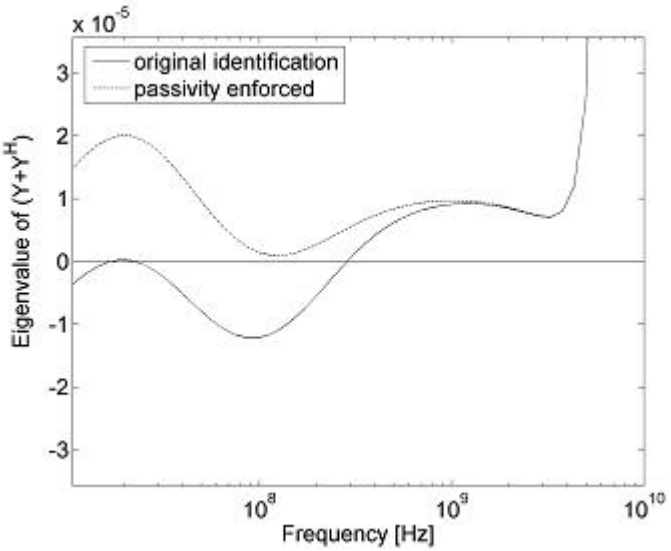

Figure 2.6: Twisted cable : passivity enforcement on the first eigenvalue.

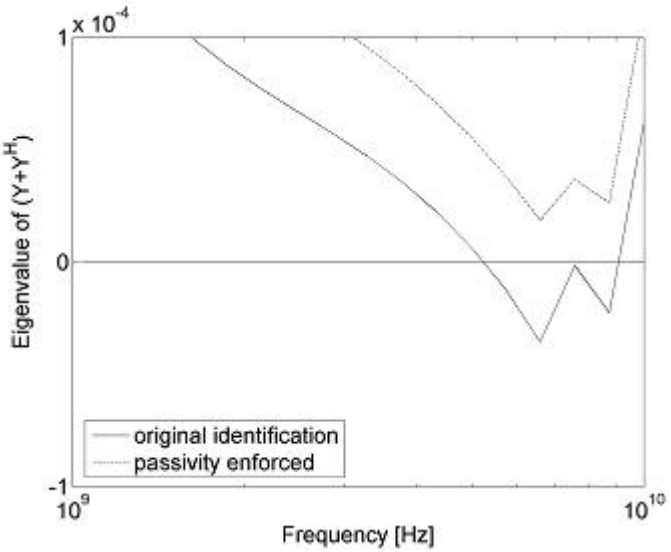

Figure 2.7: Twisted cable : passivity enforcement on the first eigenvalue.

Chapter 3

Transmission line modelling

3.1 Introduction

Due to the rapid increase of the signal frequency and decrease of the electronic component sizes within high speed electronic circuits, high-density interconnects often behaves as multiconductor transmission lines.
Therefore, accurate and efficient simulation techniques are needed not only for power systems analyses, but also for design and verification of the modern electronic circuits. In such a case, transmission line effects (delay times, crosstalk voltages, voltage overshoots on terminal devices, etc.) must not affect correct operation of these systems.
It is known in literature that the generalized Method of Characteristic (MoC) provides the most suitable model to perform transient analysis of transmission lines. Several techniques for the computation of the line responses exist (e.g. see the comprehensive reviews of Djordjevic et al. (1987) [46] and Paul (1994,1996) [47] [48]). The foremost methods are modal analysis in the time domain, modal analysis in the frequency domain, and convolution techniques that use line impulse responses.
A significant problem in the analysis of multiconductor lines is the inclusion of the terminal networks. For lossless lines with frequency-independent parameters, i.e. ideal lines, the study of the entire system (lines and terminations) can be performed in the time domain by using the modal analysis. In all other cases the analysis of the line must be necessarily performed in the frequency domain or, equivalently, in the Laplace domain. If the terminal networks are linear the entire analysis can be performed in the frequency domain and the inverse Fourier transform is used to obtain the solution in the time domain. However, this approach is not suitable for handling fast-varying signals and when the terminal networks are nonlinear (Maffucci and Miano 1999 [49]). In the general case, terminal net-

works requires a time domain analysis, whereas the line has to be modelled in the frequency domain due to the losses and/or the dispersive phenomena. Both requirements can be satisfyed by using the convolution technique. Furthermore, fast convolution algorithms can be used in the simulation of lines ended with linear networks and involving fast-varying signals as well (e.g. Lin and Kuh (1992) [50], Gordon et al (1992) [51]).
Effective time-domain simulations for multiconductor lines are achieved through convolution of the line terminal voltages with the describing time-domain input and transfer impulse responses of the line. These line responses are computed, respectively, from the Laplace-domain admittance matrix and the propagation matrix. The common problem to overcome is given by the high computational cost of time convolutions, which leads to the need to derive reduced order models. In the frequency domain, where it is natural to take into account the frequency-dependence of the line p.u.l. parameters, the model obtained from MoC is described by operators characterized by a rather complicated behavior. These operators, in particular, show a singular behavior at infinity due to the presence of irregular terms, mainly arising from the delays associated to propagation. The delay extraction allows, from one hand, to describe analytically the highly irregular and unbounded terms contained in the line impulse responses, which can be modeled through damped delayed sources and resistive multiports. On the other hand, it allows to define regular remainders which can be easily identified by means of low-order lumped circuit approximation, so lowering the computational cost of the convolutions. The most commonly adopted approaches to extract these delays are based on an asymptotic evaluation of the behavior of the frequency domain operators describing the model.
This chapter analyzes the following issues:

- the analytical evaluation of the delays as well as the corresponding damping factors. This comes from a procedure based on the theory of the perturbation of the spectrum of symmetric operators (Miano and Maffucci 2001 [52]). The exploitation of such analytical information leads to a new definition of the remainders under identification, as compared to other approaches available in literature (e.g. Elfadel et al 2002 [53], Grivet Talocia et al 2004 [54]).

- the identification process of the describing functions after the extraction of the available analytical information. A procedure consisting of a cascade of Vector Fitting [4] [26] and a further non-linear minimization, already introduced in section (1.6) is successfully applied. This allows giving general properties to the macromodel realization, also improving the accuracy. In particular, it leads to state space realizations having a diagonal matrix A with no repeated poles.

- the possibility of improving the accuracy of the propagation operator identification through the identification of optimal time delays.

The decomposition of the describing functions and the identification procedures are tested on standard examples of RLGC multiconductor transmission lines. Improvements in the identification of reduced-order lumped equivalents will be highlighted, both in the characteristic admittance matrix and propagation operator matrix.
The identification of optimal delays to be extracted from propagation operator have been tested on power transmission lines. Also in this case, results show the effectiveness of the proposed approach.

3.2 The Method of Characteristics

Let us consider a line of length d consisting of m signal conductors and a reference one. The frequency-domain distributions of currents $I(z,s)$ and voltages $V(z,s)$ along the line are solution of the telegrapher's equations:

$$-\frac{dV}{dz} = Z(s)I, \; -\frac{dI}{dz} = Y(s)V. \tag{3.1}$$

With a suitable definition of the per-unit-length (p.u.l.) impedance $Z(s)$ and admittance $Y(s)$ matrices, these equations describe the most general case of lossy multiconductor lines with frequency dependent parameters. Having defined the terminal variables as V_k, I_k, $k = 1, 2$ at the near and far end, respectively, the following equivalent multiport representation may be derived (e.g. [52]):

$$\begin{aligned} I_1(s) &= Y_c(s)V_1(s) + J_1(s), \\ I_2(s) &= Y_c(s)V_2(s) + J_2(s), \end{aligned} \tag{3.2}$$

$$\begin{aligned} J_1(s) &= H(s)[-2I_2(s) + J_2(s)], \\ J_2(s) &= H(s)[-2I_1(s) + J_1(s)]. \end{aligned} \tag{3.3}$$

Eqs. (3.2) are the network equations at the two line ends, while eqs. (3.3) describe the control laws of two controlled current sources. The characteristic admittance matrix $Y_c(s)$ and the propagation operator matrix $H(s)$ are given by:

$$Y_c(s) = \left(\sqrt{Z\,(s)^{-1}\,Y\,(s)^{-1}}\right) Y(s), \tag{3.4}$$

$$H(s) = e^{-\sqrt{Y(s)Z(s)}l}. \tag{3.5}$$

The time-domain model is obtained by reverse transforming (3.2) and (3.3), hence it involves the time convolution product between the voltage and current waveforms and the inverse transforms of (3.4) and (3.5), i.e. the line impulse responses: $y_c(t) = L^{-1}\{Y_c(s)\}$, $h(t) = L^{-1}\{H(s)\}$. This model is extremely accurate since

it fits naturally the propagation: for instance, when port 2 is matched $J_1 = 0$ and the model exactly provides the characteristic admittance as the input admittance at port 1. Nevertheless it also presents a couple of weak points:
(i) the difficult evaluation of the impulse responses;
(ii) the high computational cost of the time convolutions.
For these reasons, the literature has proposed semi-analytical approaches which evaluate in an accurate manner such functions; at the same time, efficient reduced order models have been proposed to lower the computational cost. The crucial point to overcome both the problems is the extraction of the delayed terms involved in the propagation operator $H(s)$. Regarding to this issue, it is of remarkable importance the possibility for the propagation operator to be diagonalized as follows:

$$H(s) = U(s)diag\left(e^{-ds\sqrt{\lambda_1(s)}}, ..., e^{-ds\sqrt{\lambda_n(s)}}\right) U^{-1}(s) \tag{3.6}$$

Where $\lambda_i(s)$ and the columns $u_i(s)$ of matrix $U(s)$ are, respectively, the eigenvalues and the eigenvectors of the matrix:

$$\Lambda(s) = \frac{Y(s)}{s}\frac{Z(s)}{s} \tag{3.7}$$

3.3 Identification of the describing operators

3.3.1 The characteristic admittance matrix Y_c

The identification of the characteristic admittance matrix $Y_c(s)$ is a problem quite similar to the identification of any matrix of smooth frequency responses describing delayless distributed multiports.
In addition, valuable information on its structure can be exploited to simplify the identification process. In such a case, the characteristic admittance may be decomposed in a principal part and a remainder:

$$Y_c\left(s\right) = Y_{cp}\left(s\right) + Y_{cr}\left(s\right) \tag{3.8}$$

where $Y_{cp}\left(s\right)$ is the leading part as $s \to \infty$, while $Y_{cr}\left(s\right)$ is a low-pass function for $s \to \infty$. The extraction of the principal part of $Y_c(s)$ is straightforward, since it corresponds to the characteristic admittance of an ideal lossless line described by p.u.l. inductance and capacitance matrices given by $L_\infty = \lim_{s\to\infty}\left(Z(s)/s\right)$ and $C_\infty = \lim_{s\to\infty}\left(Y(s)/s\right)$. After this decomposition only $Y_{cr}\left(s\right)$ needs to be identified with a rational (low-pass) function.
The identification of the matrix Y_c (or Y_{cr}, when the asymptotic behaviour of the p.u.l. inductance and capacitance is known) can be accurately achieved by using a common pole set:

$$Y_c^{(ij)}(s) = \sum_m \frac{c_m^{(ij)}}{s - p_m} + d^{(ij)}. \tag{3.9}$$

Gustavsen et al (1999) [55] provided the following intuitive explanation of this. The Y_c matrix might be diagonalized as follow:

$$Y_c(j\omega) = T(j\omega)\lambda(j\omega)T^{-1}(j\omega), \tag{3.10}$$

where $\lambda(j\omega)$ is the diagonal matrix holding the modes of Y_c:

$$\lambda(j\omega) = \begin{pmatrix} \lambda_1(j\omega) & \dots & 0 \\ \vdots & \ddots & 0 \\ 0 & \dots & \lambda_n(j\omega) \end{pmatrix} \tag{3.11}$$

Let be T_k is the k-th column of T, and T_k^{-1} is the k-th row of T^{-1}, (3.10) may be rewritten as:

$$Y_c = \sum_{k=1}^{n} T_k \lambda_k T_k^{-1} = \sum_{k=1}^{n} (T_k T_k^{-1})\lambda_k. \tag{3.12}$$

The frequency variations of $T_k T_k^{-1}$ are the same of those of $\lambda_k(j\omega)$. This indicates that the degrees of freedom provided by the residues is sufficient to approximate the whole matrix Y_c, by using only the poles of each $\lambda_k(j\omega)$. Note that the modal decomposition of Y_c is not actually needed by the identification process.
For large matrices, an estimation of the pole set is given by the poles of $\sum_{k=1}^{n} \lambda_k$. Since the sum of the eigenvalues of a matrix equals its trace:

$$\sum_{k=1}^{n} \lambda_k = \sum_{k=1}^{n} Y_c^{(kk)}, \tag{3.13}$$

even in this case, it is not necessary to evaluate the matrix $\lambda(j\omega)$.

3.3.2 The propagation operator $H(s)$

Due to its structural properties the identification of the propagation operator is the real challenge in modeling transmission lines. The structure of the operator $H(s)$ is more complicated as compared to $Y_c(s)$ mainly due to the presence of the propagation delays. If it were directly subjected to a rational approximation, expansions of high order would be required.
For this reason, also for $H(s)$, we look for extracting a part which may be analytically computed, leading to the definition of a regular remainder identifiable with a low order expansion.

Long interconnects modelling

For many cases of practical interest, which include interconnects with frequency-independent parameters (RLGC lines) and a large class of lines with frequency-dependent parameters (such as the lines with dispersive dielectrics), the following

expansion for $s \to \infty$ of eigenvalues and eigenvectors holds [52]:

$$\lambda_i(s) = \lambda_i^{(0)} + \frac{\lambda_i^{(1)}}{s} + ..., \quad u_i(s) = u_i^{(0)} + \frac{u_i^{(1)}}{s} + ... \tag{3.14}$$

where the zero-order terms λ_i^0 and u_i^0 are, respectively, the eigenvalues and eigenvectors of the high-frequency limit of matrix (3.7):

$$\Lambda_0 = C_\infty L_\infty \tag{3.15}$$

where $L_\infty = \lim_{s\to\infty}(Z(s)/s)$ and $C_\infty = \lim_{s\to\infty}(Y(s)/s)$. Now, let us neglect the fact that the time delay T_i associated to the i^{th} TEM mode propagating along the line is actually frequency dependent, and give the following definition:

$$T_i = d\sqrt{\lambda_i^{(0)}}. \tag{3.16}$$

We can introduce the matrix U_0 as the u_i^0 eigenvectors matrix, and define diagonal matrices D and M containing respectively, the delay factors and the damping factors associated to such delays as:

$$D = diag[\exp(-sT_i)], \tag{3.17}$$

$$M = diag[\exp(-\mu_i T_i)]. \tag{3.18}$$

Then, in all cases for which (3.14) holds, we can write:

$$U_0^{-1} H(s) U_0 = D\left[M + Q\left(s\right)\right] \tag{3.19}$$

where the $Q(s)$ matrix accounts for the dispersion phenomena, which would vanish in the so called distortionless "Heaviside" condition. Note that for the ideal lossless case $Q(s) = 0$ and $M = I$ (identity matrix). It is worth noting that the damping coefficients μ_i could be evaluated from the knowledge of the first order term λ_i^1 in the expansion of $\lambda_i(s)$ [52]:

$$\mu_i = \frac{\lambda_i^{(1)}}{2\lambda_i^{(0)}}; \tag{3.20}$$

this approach represents the generalization to multiconductor case of the well-known expression of the damping coefficient for a two-conductor RLGC line $\mu = 1/2\left(R/L + G/C\right)$.
Expression (3.19) is well suited to the system identification since all the information related to propagation delays is explicitly accounted in matrix D . Moreover, the analytical evaluation of damping factors in matrix M leaves only matrix $Q(s)$ to be determined.
Finally, it is important to stress that a similar procedure may be adopted also for another class of dispersive lines, as for example the lines with pronounced skin

effect. In such a case the starting point is the expansion in Laurent series in the neighborhood of $s \to \infty$ by powers of $1/\sqrt{s}$ [52].
The definition of a regular remainder to be identified with a low order expansion, may be achieved by two different approaches. Such remainder is then identified by using a common pole set, like $Y_c(s)$ in eq. (3.9).
First approach is here called "Subtracting approach". It has been presented, for instance, by Miano and Maffucci in [52], and removes directly a principal part from the overall operator:

$$H(s) = H_p(s) + H_r(s) \tag{3.21}$$

with $H_p(s)$ given by:

$$H_p(s) = U_0 M D U_0^{-1} = U_0 diag[-(\mu_i + s)T_i] U_0^{-1}, \tag{3.22}$$

so defining a regular remainder $H_r(s)$ vanishing as $1/s$ for $s \to \infty$, which has to be identified. With this approach the implementation is straightforward: $H_p(s)$ may be realized by a network of pure delay elements and constant gains; $H_r(s)$ by the reduced system as obtained by identification. It is important to note that $H_r(s)$ contains the contributions of m different modes, each of which is associated with its own delay time T_i. In particular, since its corresponding time-domain transform $h_r(t)$ has to be zero for $0 \leq t \leq T_{\min}$, where T_{min} is the time delay associated to the fastest mode, it is extremely convenient to pursue the identification of:

$$\tilde{H}_r(s) = e^{sT_{\min}}[H(s) - H_p(s)], \tag{3.23}$$

rather than of $H_r(s)$ as defined in (3.21).
A different way to define the remainder is based on delays factorization. We refer to it as "Factorizing Approach". From (3.19), in fact, it is possible to define the following expression (Grivet-Talocia et al 2004 [54]):

$$M + Q(s) = D^{-1} U_0^{-1} H(s) U_0 \tag{3.24}$$

Note that $Q(s)$ is a regular remainder. Once $M + Q(s)$ has been identified, the propagation operator $H(s)$ is easily obtained by the following manipulation:

$$H(s) = U_0 D [M + Q(s)] U_0^{-1} \tag{3.25}$$

From (3.24) it is evident how the implementation of $H(s)$ requires the reassembling of the contribution of the m modes each one with its own delay. Anyway, since it is possible to compute matrix M analytically, a new definition may be introduced for the remainder to be identified (de Magistris et al 2005 [56]):

$$H_r(s) = M^{-1} D^{-1} U_0^{-1} H(s) U_0 - I \tag{3.26}$$

Such a definition can improve the whole identification process by exploiting the analytical knowledge of the damping matrix M, whereas definitions (3.23) or (3.24) leave this information in the reminder to be identified.

Power lines modelling

In the modelling of some power lines, the usage of a constant transformation matrix U_0 to diagonalize the propagation function $H(s)$ may give inaccurate results, due to a quite pronounced frequency dependent behaviour. An efficient procedure, which enables to take into account even strongly frequency dependent transformation matrix and widely different modal time delays, was introduced by Gustavsen et al (1999) in [55] and is called "Universal Line Model". It involves two steps: the modal domain fitting of propagation matrix $H(s)$ and the phase domain fitting of $H(s)$. Modal domain fitting means that $H(s)$ is diagonalized (3.6) and its modal components are identified with a rational approximation plus a single time delay. Phase domain fitting means the identification of whole matrix $H(s)$ by taking the poles of all modes (as previously found in the modal domain fitting) and their time delays as known quantities.
Now, we describe the modal domain fitting of $H(s)$. Similarly to (3.12), we have:

$$H = \sum_{m=1}^{n} (U_m U_m^{-1}) e^{-\gamma_m l} = \sum_{m=1}^{n} (U_m U_m^{-1}) e^{-\chi_m l} e^{-j\omega\tau_m} \tag{3.27}$$

Note that we have extracted a constant delay, τ_m, for each mode. Factors $e^{-\chi_m l}$ are still frequency dependent. Each mode $e^{-\gamma_m l}$ may be written in the form:

$$h^m(\omega) = e^{-\gamma_m l} = e^{-\left(\alpha_m(\omega) + j\frac{\omega}{v_m(\omega)}\right) l}, \tag{3.28}$$

where α_m is the attenuation, v_m is the velocity and l is the line length. Lossless time delays τ_m (which correspond to (3.16)) may be written as:

$$\tau_m = \frac{l}{v_m(\omega \to \infty)}. \tag{3.29}$$

After that modes have been found and a time delay is extracted from each mode, we find their poles $\{p_{km}\}$ (for instance, through the Vector Fitting algorithm):

$$h_m e^{j\omega\tau_m} = e^{\chi_m l} = \sum_k \frac{c_{km}}{j\omega - p_{km}}. \tag{3.30}$$

Now, the phase domain fitting has to be performed. It involves the identification of residues of the following expansion:

$$H_{ij}(j\omega) \approx \sum_{m=1}^{n} \left(\sum_{k=1}^{N} \frac{(c_{mk})_{ij}}{j\omega - p_{mk}} \right) e^{-j\omega\tau_m}. \tag{3.31}$$

Writing the (3.31) for several frequencies, an overdetermined linear matrix equation of the form

$$AX = B, \tag{3.32}$$

is found. The unknown residues ($\{(c_{mk})_{ij}\}$) are in X. Each row in A and B corresponds to a frequency point, and each column in X and B corresponds to an element of H. Equation (3.32) is solved as a least squares problem. It should be noted that all poles $\{p_{mk}\}$ are present in all elements H_{ij} of the fitted H matrix. This enables a columnwise realization for H, leading to computational savings in the implementation of the time domain model.
Note that, if the eigenvalues of H were calculated using a constant, real transformation matrix evaluated at a high frequency (e.g. 1 MHz), the resulting eigenvalues would be different from the accurate ones. The identification gives different poles as well. However, in some cases, these displacements of the poles are known to be slight and can be compensated in the calculation of the residues. In such cases, it is advantageous to use a constant transformation matrix, since this avoids the problem of artificial mode switchovers, so eliminating the need for a "tracking routine" (Wedepohl et al 1996 [57]) or special diagonalization routines (Marti 1988 [58], Wedepohl et al 1996 [57]).
In the actual implementation of ULM, modes with nearly equal delays are lumped together in order to obtain a more compact model [55].

3.4 On the evaluation of time delays

For some particular applications (like power transmission lines) lossless time delays (3.16), may be difficult to evaluate according an expansion like (3.14). In such a case, they may be evaluated directly from the magnitude of the propagation function (Gustavsen and Semlyen 1998 [59]).
Since the function $h_m(\omega)$ may be also decomposed as follows:

$$h_m(\omega) = h_{\varphi m}(\omega) e^{-j\omega\tau_m}, \tag{3.33}$$

where $h_{\varphi m}$ is a minimum phase shift function, from (3.28) it results:

$$-\frac{\omega}{v_m(\omega)} l = \angle h_{\varphi m}(\omega) - \omega\tau_m. \tag{3.34}$$

The (3.34) enables the evaluation of the time delay τ_m once $\angle h_{m\varphi}(\omega)$ is known:

$$\tau_m = \tau_m^a + \Delta\tau = \frac{l}{v_m(\omega)} + \frac{\varphi(\omega)}{\omega}. \tag{3.35}$$

The phase angle $\varphi(\omega) = \angle h_{\varphi m}(\omega)$ may be calculated from the magnitude function $|h|$, by using the Bode phase-integral theorem:

$$\varphi(\omega) = \frac{\pi}{2} \frac{d(\ln|h(\omega_1)|)}{d(\ln\omega_1)}\bigg|_{\omega_1=\omega} + \Delta(\omega), \tag{3.36}$$

where

$$\Delta(\omega) = \frac{1}{\pi} \int_{-\infty}^{+\infty} \left(\left| \frac{d(\ln|h|)}{du} \right| - \left| \frac{d(\ln|h|)}{du} \right|_{u=0} \right) \ln\left(\coth\frac{|u|}{2} \right) du, \tag{3.37}$$

and

$$u = \ln \frac{\omega_1}{\omega}. \tag{3.38}$$

Note that the theorem gives an analytical expression of the phase angle $\varphi(\omega)$ of a minimum phase shift function as a function of logarithm of its magnitude $|h|$. The integral of (3.4) spans over the entire frequency axis, requiring always the magnitude function $|h(\omega_1)|$ at any ω_1, in order to evaluate exactly the phase angle at a single frequency point ω. In the practical implementation, the integral is evaluated numerically on a limited frequency interval. For this application, a quite accurate approximation is usually achieved when it is taken over a frequency range that spans at least two decades below and above ω.
If the minimum phase angle $\varphi(\omega)$ is accurately evaluated, the time delay (3.35) is independent from the frequency point ω chosen. In practice, evaluating the integral of (3.4) on a limited frequency range around ω, the obtained approximation is dependent from ω.
Note that integrand in (3.4) is singular for $u = 0$, and the integration has to be intended in the sense of Cauchy principal value (Poularikas 1996 [60]):

$$\int_{-\infty}^{+\infty} = \lim_{\varepsilon \to 0^+} \left[\int_{-\infty}^{-\varepsilon} + \int_{\varepsilon}^{+\infty} \right] \tag{3.39}$$

The factor $ln(coth(|u|/2))$ peaks when $u = 0$ (i.e. $\omega_1 = \omega$), the phase angle at a given ω mostly depends by the magnitude slope around ω [60].
The numerical implementation of (3.36), (3.4) substitutes the limit $\varepsilon \to 0$ by a given value of the sampling interval and the limit to infinite by a given value of the upper/lower frequency. We perform the numerical integration of () by using an uniform sampling of the integral, i.e. $\omega_{1j} = j\Delta\omega$, where $j \in \{-N, \ldots, -1, 1, \ldots, N\}$ and Δ is assumed as a constant, which corresponds to $u_j = j\Delta$. This gives a proper approximation of the integrand of (3.4) in the sense (3.39), since the origin $u = 0$ is positioned exactly at the center of the sampling interval. Such a goal is simply achieved generating the vector `w` containing the angolar frequencies by means of the Matlab command `logspace`.
The following shows a Matlab code for calculating the phase angle of a minimum-phase shift function by (3.36),(3.4). It is assumed that `absH` contains the magnitude function, given at `Ns` frequency samples. The code calculates the phase angle at the j^{th} frequency sample.

```
phase1=(pi/2)*log((absH(j+1)/absH(j-1)))/(log(w(j+1)/w(j-1)));
phase2=0;
term2=log((absH(j+1)/absH(j-1))) /(log(w(j+1)/w(j-1)));
for k=2:Ns-1
    term1=log(absH(k+1)/absH(k-1)) /(log(w(k+1)/w(k-1)));
    if k~=j
```

```
        phase2=phase2+
        abs(term1)-abs(term2))*log(coth(abs(log(w(k)/w(j)))/2))*
        log(w(k+1)/w(k));
    end
end
phase2=phase2/pi;
phi(j)=(phase1-phase2); %Phase angle [rad]
```

3.5 Identification of optimal time delays

We have already seen that the identification of $H(s)$ is somewhat challenging since a low order approximation is achievable only with the accurate evaluation and extraction of the modal time delays (3.23), (3.24), (3.25).
In the case of power transmission lines, a very accurate identification approach (ULM [55]) requires the modal domain fitting of $H(s)$, i.e. the identification of its modal components with a rational approximation plus a single time delay. These time delay may be evaluated through the formula (3.35), which is based on the possibility of reconstructing a minimum phase angle by means of the Bode phase-integral theorem (3.36). However, it has been shown that the rms-error of the rational approximation of each modal component has a minimum for a time delays greater than the lossless (e.g. Gustavsen 2004 [61]).
In this section we describe an approach which improves the approximation of the whole $H(s)$ matrix by means of the identification of optimal time delays.
To motivate this approach, we consider as example of identification, the propagation function of a single overhead line. In such a case the propagation operator $h(s)$ is a scalar function, so the diagonalization (modal decomposition) in (3.24) does not apply.
After the delay extraction, the delayless propagation operator $p(s)$ can be identified by means of the VF algorithm:

$$p(s) = h(s)e^{s\tau} \cong \left(\sum_{m=1}^{N} \frac{r_m}{s - a_m} \right) \tag{3.40}$$

We will show that the extraction of a time delay different from (3.16) can give a more accurate final approximation. In this case the function to be subject to a rational approximation is no longer a minimum phase shift function.
A practical example is given in fig. (3.5), where the propagation function $h(s)$ of a 50 km long overhead line has been subjected to a rational approximation (eight poles) over the frequency interval [1 Hz, 10 MHz]. The figure shows the comparison between the extraction of the lossless time delay τ_0 and a time delay $\tau_1 > \tau_0$. Stability has been enforced by the use in the fitting process of only negative real part poles. It is seen that compensation with the time delay $\tau_1 > \tau_0$, gives a less

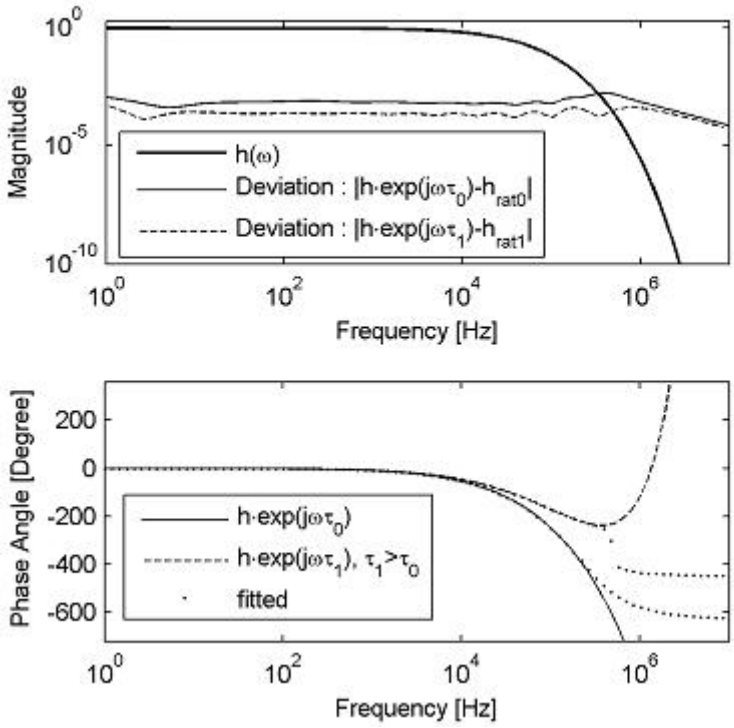

Figure 3.1: Identification of a propagation function, after extraction of lossless time delay τ_0 and $\tau_1 > \tau_0$

negative phase angle for that range of frequencies where the magnitude of the original function is not negligible yet. This enables a more accurate approximation without increasing the order: the rms-error of the approximation performed extracting τ_1 is 2.55×10^{-4}, whereas it is 7.76×10^{-4} when τ_0 is extracted.

In fig.(3.5), a time delay τ_2, with $\tau_1 > \tau_2 > \tau_0$, has been extracted. It is shown that the eight-poles function cannot capture perfectly the phase angle, giving an approximation less accurate than that one shown in fig. (3.5). In this case the rms-error is 5.75×10^{-4}. The sixteen-poles approximation is very accurate, giving the rms-error 4.39×10^{-6}. Moreover, when time delay $\tau_1 > \tau_2$ is extracted, the sixteen-poles approximation loses accuracy, giving a rms-error comparable to the eight-poles approximation: 9.81×10^{-5}.

Similar considerations, which hold also for each modal component of a matrix propagation function $H(s)$, suggest that time delay which gives least rms-error is greater than lossless one, and depends from the order of the approximation. The lower is the order, greater is the time delay which minimizes the rms-error.

It is therefore desirable to use an optimization procedure which computes the delay that minimizes the rms-error for a given order of approximation.

A very accurate procedure for including modal time delays in the optimization

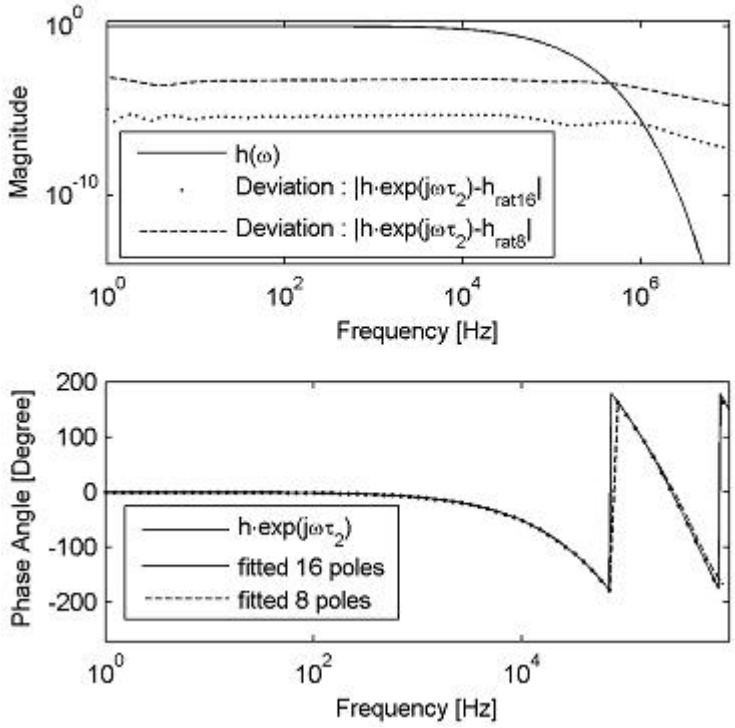

Figure 3.2: Identification of a propagation function after extraction of a time delay τ_2, with $\tau_1 > \tau_2 > \tau_0$

process was introduced by Gustavsen (2004) [61] by combining Vector Fitting (VF) with Brent optimization method. The basic idea is to search for the time delay which gives the smallest possible rms-error of (3.40). Its practical implementation requires writing a routine which calculates the rational approximation and its rms-error for a given time delay. An external optimization loop is then used to minimize such an objective function.

De Tommasi and Gustavsen (2006) [22] found an alternative approach based on the fitting of the magnitude of the modal responses with minimum phase shift functions, followed by a final optimization of the time delay. This avoids the need for repeatedly fitting the response with rational functions, thereby giving some scope for speed improvement. On the other hand, this approach may give less accurate results than the previous one.

3.6 Minimum phase shift fitting and optimal time delay identification

This section shows the approach developed by De Tommasi and Gustavsen (2006), based on the fitting of the magnitude of the modal responses with minimum phase shift functions, followed by the identification of the time delay.
We have already seen that after the operator $H(s)$ has been diagonalized, terms $\{h_i^m(s)\}$ of the diagonal matrix $H^m(s)$ needs to be fitted with a rational function plus a time delay. One of the existing EMTP line models (Marti 1982) is based on magnitude fitting of the propagation function using a minimum phase shift function plus a single delay that is subject to final optimization. The fitting procedure given by Marti (1982) in [21] is based on asymptotic fitting which results in high orders and thereby slower time domain simulations.
De Tommasi and Gustavsen (2006) developed a modified version of VF to achieve a low order fitting. Standard VF requires knowledge about the both magnitude and phase of the function to be fitted, whereas this new formulation of the algorithm (described in chapter 1), fits the magnitude of a frequency responses giving a minimum phase shift function.

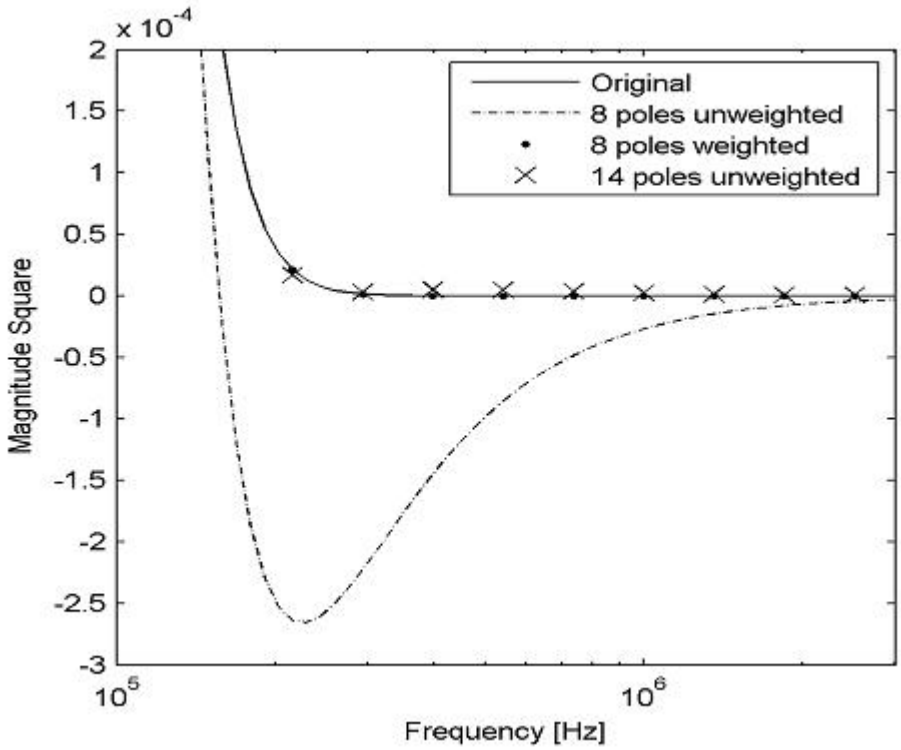

Figure 3.3: Overhead line : identification of the magnitude square of a modal component $h(s)$ of $H(s)$

First step of the magnitude fitting is the fitting of the magnitude square function and the correction of the rational function to remove its negative values. Fig. (3.3) shows the identification of the magnitude square of the ground mode of a 50 km three phase overhead line. The function has been fitted with $N = 8$ poles without any weighting for the LS solution. It is seen that a negative undershoot results with minimum value -2.66×10^{-4}. Such undershoot will result in the rational approximation having at least one conjugate couple of purely imaginary zeros. These zeros are located where the approximation crosses the zero line (in this example they are at 1.57×10^5 Hz). Also shown in fig. (3.3) is the result achieved by placing a weight of 10^4 for the samples between 1.49×10^5 and 9.40×10^5 Hz. This is seen to remove the existence of negative values.

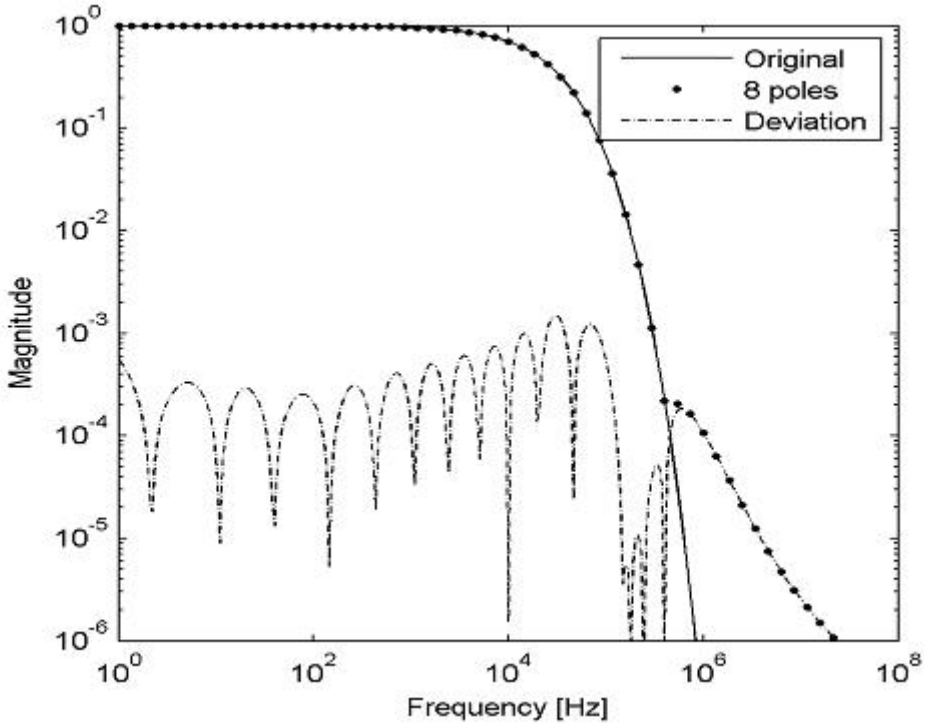

Figure 3.4: Overhead line : identification of the magnitude of a modal component $h(s)$ of $H(s)$

From the magnitude square fitting (which has no imaginary zeros) is recovered the minimum phase shift approximation of $h(s)$, see fig. (3.4).
Note that the deviation $\Delta(f)$ shown in fig. (3.4) is the distance between the two magnitude functions:

$$\Delta(f) = ||h(j2\pi f)| - |h_{fit}(j2\pi f)||\,, \tag{3.41}$$

where h is the original function and h_{fit} the eight poles approximation.

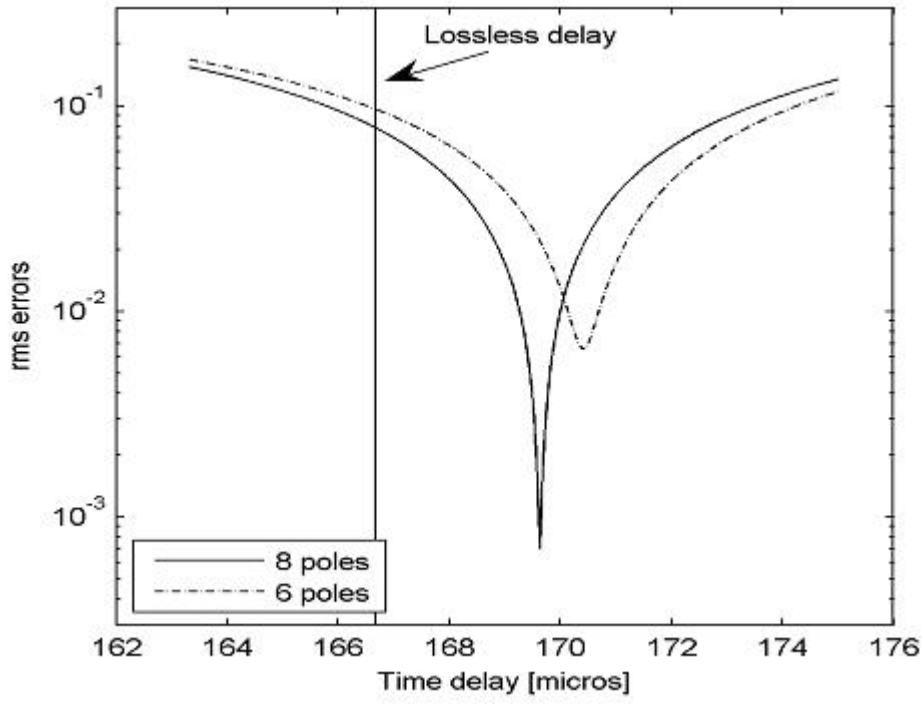

Figure 3.5: Overhead line : identification of the magnitude of a modal component $h(s)$ of $H(s)$

After that the magnitude of $h(s)$ has been fitted with a minimum phase shift function, a single time delay has to be associated. Fig. (3.5) shows that the minimum rms-error occurs for a time delay greater than $\tau_0 = 50 \times 10^3/3 \times 10^8 = 166.67\mu$s (lossless time delay). In agreement with [61], we find that the optimal time delay τ_{opt} becomes smaller as the order N of the approximation increases. The rms-error of the approximation obtained by associating a delay $\tau \neq \tau_{opt}$ to the minimum phase shift approximation of $|h(s)|$ is significantly greater than the rms-error of (3.40). However, working with several overhead line having different length, we verified that the minimum rms-error reached through the identification of τ_{opt} is lower than the rms-error of (3.40) with $\tau = \tau_0$ (lossless time delay extraction). This justifies the usage of the proposed procedure with such kind of dataset.
The delay which minimizes the rms-error is quickly evaluated by means of MATLAB function `fminbnd` [62]. This avoids usage of manual frequency sweeping.

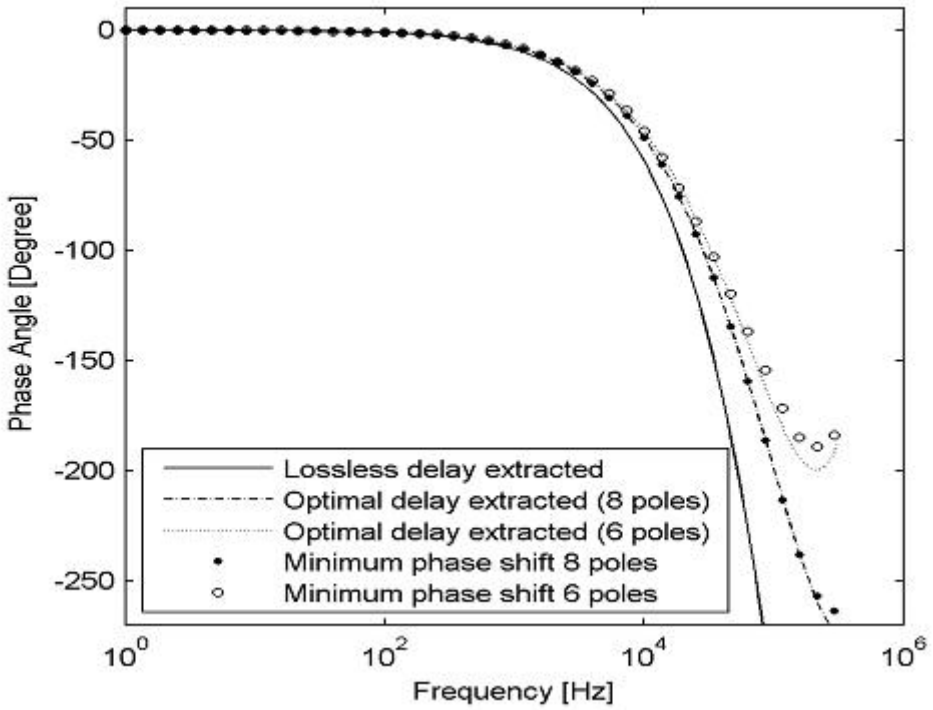

Figure 3.6: Overhead line : phase angle comparison

Fig. (3.6) compares the phase angles of the minimum phase shift rational functions with the phase angle that results when multiplying the original propagation function $h(s)$ with a factor $e^{-s\tau}$, when τ has been optimized. Clearly a very good match is achieved. Since both the magnitude and phase angle have now been fitted to a high accuracy, one can conclude that the modes h_i^m can be fitted accurately using a minimum phase shift function plus an optimized time delay, which was also the basic idea in [21].
Now, let us observe that if the magnitude square approximation approximation gives some conjugate couples of imaginary zeros, they can be replaced with real pairs, by multiplying by j. This remove the undesired negative undershoot, but the rms-error can increase substantially around those frequencies. Instead a proper weighting strategy avoids, or at least greatly reduces negative undershoots, so improving the final magnitude approximation. However, since complete elimination of negative undershoots cannot be guaranteed for any case by weighting, the presence of imaginary zeros must be always checked and removed prior to recover the final model.

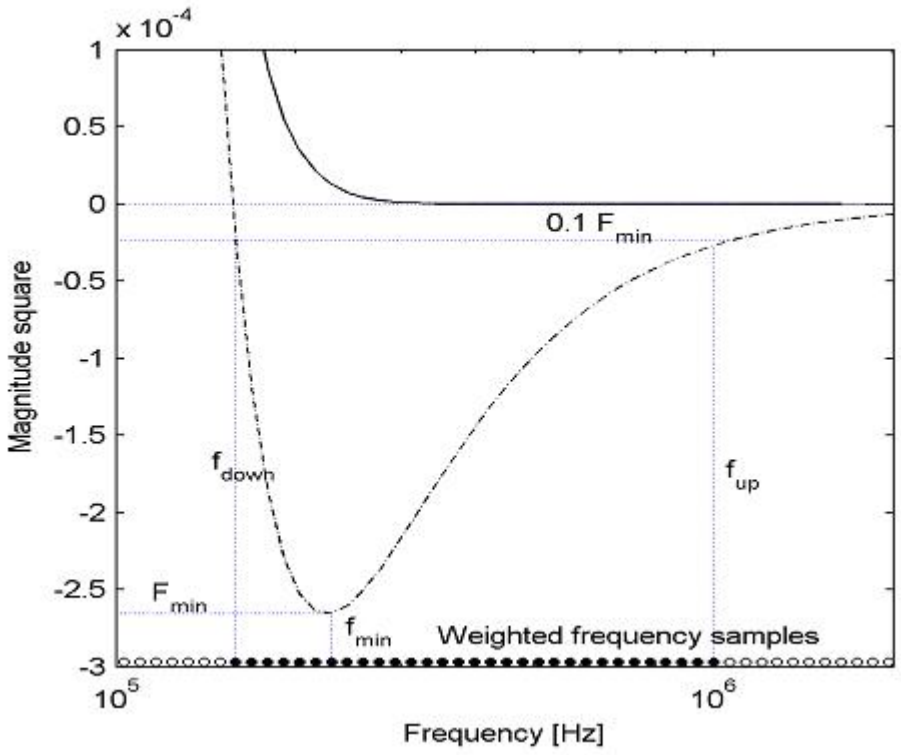

Figure 3.7: Overhead line : weighting criterion

We found the following weighting criterion which improved the approximation of several overhead line datasets. First, we have to determine the frequency band to be weighted. The magnitude square function is fitted with unitary weights and it is checked if the approximation takes negative values. If this happens, the following procedure is undertaken. From the frequency response is identified the point of minimum (f_{min}, F_{min}), see fig. (3.7). Also is identified the frequencies f_{down}, where the approximation takes the first negative value, and f_{up}, where the magnitude is 10% of $\|F_{min}\|$. Then, the function is refitted when weighting the N_x samples between f_{down} and f_{up} with the quantity:

$$w = \alpha \frac{N_s}{N_x} \frac{1}{|F_{\min}|}, \tag{3.42}$$

where α is a user-defined parameter (usually ranging from 2 up to 10), and N_s is the total number of frequency samples.

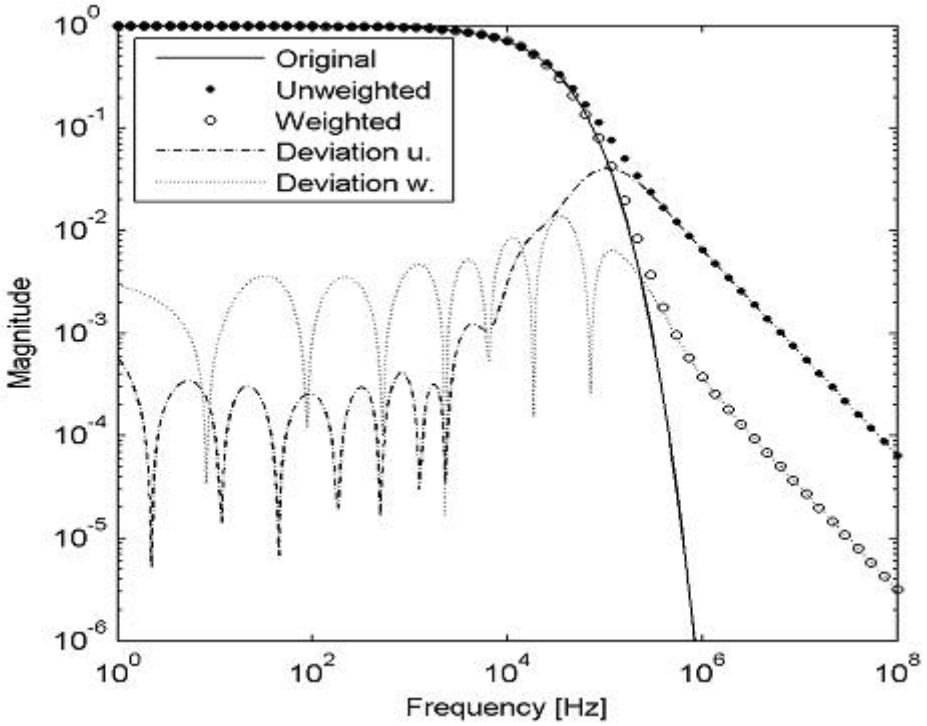

Figure 3.8: Overhead line : identification comparison, 6th order both weighted and unweighted

Fig. (3.8) shows a comparison between two sixth order approximations. The first one is obtained from an unweighted magnitude square approximation which gives the couple of imaginary zeros $\pm j9.10 \times 10^5$ (taking a negative minimum of 4.44×10^{-4} at 215 kHz). These imaginary zeros are replaced by the real couple $\pm 9.10 \times 10^5$, before recovering the final approximation of the magnitude. The second one comes from a weighted magnitude square fitting, assuming $\alpha = 3$ in (3.42). In this case the magnitude square rational approximation gives two very close couple of imaginary zeros: $\pm j2.48 \times 10^6$, $\pm j2.55 \times 10^6$, resulting in a negative minimum of -5.68×10^{-10} at 398 kHz. By changing the imaginary zeros into their real counterparts before recovering the magnitude fitting, the introduced perturbation is much smaller than in the first case. It is seen that the final result is more accurate around those frequencies where the imaginary zeros were located. It is also seen that the weighting increases the rms error at low frequencies, resulting in a more uniform rms error level.

3.6.1 Discussion

In this section we compare different delay optimization processes, as they are carried out in conjunction with different fitting approaches. Figure (3.9) refers to the ground mode of a 10 km long single cable system. It shows the rms-error as function of time delay, when time delay is associated to previously identified minimum phase shift functions.
In particular:

- "Bode Fitting + NLLS" uses the asymptotic fitting of magnitude function as described in (1.5.1) to obtain poles and zeros which are further refined using a non linear least square procedure. We implemented a zeros optimization scheme based on the Gauss-Newton algorithm. It takes as initial values the poles and zeros determined by asymptotic fitting and optimizes simultaneously the whole set of zeros to minimize the rms error. Poles are taken as fixed in this process. We also found that similar results in accuracy can be achieved taking the zeros as fixed and optimizing the poles.

- "Phase reconstruction + VF" uses Bode phase integral theorem (3.36) to reconstruct a minimum phase shift function which is then multiplied by the time delay before fitting with the Vector Fitting algorithm. Note that the formula (3.36) is repeatedly used at each frequency where samples of the original function are assigned.

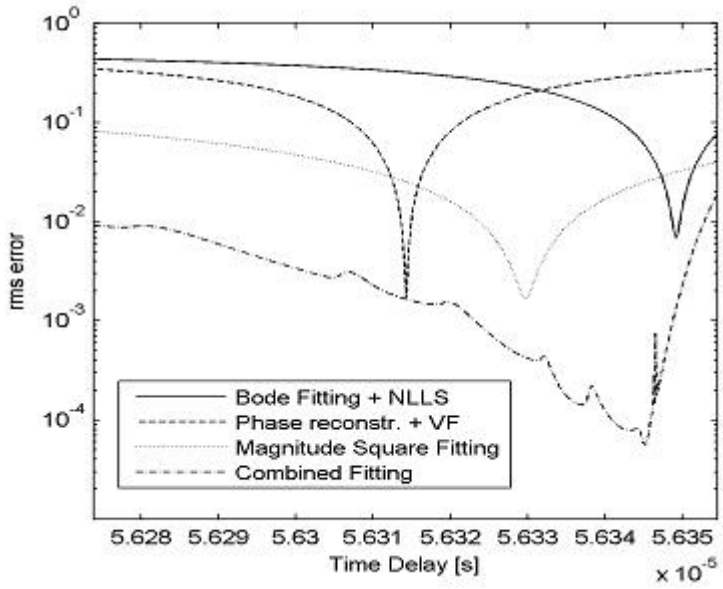

Figure 3.9: Delay optimization performed in conjunction with different fitting approaches

- "Magnitude square fitting" uses the minimum phase shift fitting approach given by De Tommasi and Gustavsen (2006), described in section (3.6). It requires the fitting of the magnitude square function through a modified version of the Vector Fitting algorithm.

- "Combined fitting" uses the procedure given by Gustavsen (2004) in [61] which identifies a new rational approximation for each time delay extracted.

Fig. (3.9) shows the general case where the combined fitting gives the most accurate approximation. We also found several cases where this approach does not give a significant improvement of accuracy with respect to that based on the magnitude square fitting.
It is seen that the old procedure given by Marti (1982) in [21] and based on the row Bode-fitting approach gives the least accurate approximation. We found that this is a quite general result.
Note that although phase reconstruction and magnitude square fitting give the same accuracy, time delays which minimize respective approximations are different. This means that starting minimum phase shift functions have different phase angles. In fact, a minimum phase angle is uniquely defined only when the magnitude of the function is assigned at any frequency, whereas the approximated functions are evaluated on a limited frequency band.

Chapter 4

Applications and case studies

4.1 Introduction

In this chapter we consider some applications of the described identification algorithms, which will be developed more deeply than the examples included in previous chapters.
First of all, we will show the effectiveness of such reduced order models and their accuracy through some time domain simulations arising from different and concrete electrical engineering problems. Then, we will address the black-box modelling of a large class of long interconnects operating in non-TEM conditions.
In detail, case studies considered are:

- The evaluation of crosstalk voltage in interconnects modelled as multiconductor transmission line. This issue is related with the signal integrity analysis in the electronic packaging.

- The analysis of the induced sheath voltage in a cable system for power transmission. This is needed in the analysis of the behaviour of the dielectric insulation under overvoltage conditions.

- The identification of passive reduced order models of interconnects operating in non-TEM conditions. In such case, bands of passivity violations due to some known inconsistencies of the full-wave model describing the interconnects, are successfully corrected after the identification stage.

Table 4.1: Interconnect 1 : p.u.l. parameters

$$R = \begin{pmatrix} 41.6667 & 0 & 0 \\ 0 & 41.6667 & 0 \\ 0 & 0 & 41.6667 \end{pmatrix} \frac{\Omega}{m}$$

$$L = 10^{-5} \begin{pmatrix} 0.2417 & 0.0694 & 0.0639 \\ 0.0694 & 0.2361 & 0.0694 \\ 0.0639 & 0.0694 & 0.2417 \end{pmatrix} \frac{H}{m}$$

$$G = 10^{-3} \begin{pmatrix} 0.5859 & 0 & 0 \\ 0 & 0.5859 & 0 \\ 0 & 0 & 0.5859 \end{pmatrix} \frac{S}{m}$$

$$C = 10^{-10} \begin{pmatrix} 0.2099 & -0.1235 & -0.0401 \\ -0.1235 & 0.2623 & -0.1235 \\ -0.0401 & -0.1235 & 0.2099 \end{pmatrix} \frac{F}{m}$$

4.2 Crosstalk voltage evaluation in long interconnects

In the modern electronic packaging, several interconnects are routed in parallel over electrically significant distances. The prediction of their electrical performances requires accurate and numerically efficient estimates of signal crosstalk voltages. Although there exists some crosstalk formulas, they are only applicable to two conductor lines and only when the dielectric medium is homogeneous. Both near-end and far-end crosstalk voltages need to be estimated for the general case of multiconductor coupled transmission lines. The effects of velocity dispersion on crosstalk voltages, which are functions of signal rise times, have to be included in the analysis.
We consider three test cases. First two refer to transmission lines characterized by frequency-independent p.u.l. parameters, whereas the third refers to a line with frequency-dependent parameters.
Both regular parts of propagation function and characteristic admittance have been identified with a common pole set by means of the matrix fitter package `mtrxfit.m`, available at `http://www.energy.sintef.no/Produkt/VECTFIT/`.

4.2.1 Case study 1

The first case analyzed is the four-conductor TL characterized by the frequency-independent p.u.l. parameters of table (4.1). The line length is 1 m.
This case shows an appreciable difference in the values of the delay times associated with the TEM modes, which are given in table (4.2), along with the computed damping coefficients.

Table 4.2: Interconnect 1 : delay times and damping coefficients

	Mode 1	Mode 2	Mode 3
τ_i	3.67 ns	6.67 ns	8.15 ns
μ_i	$8.75 \cdot 10^7 s^{-1}$	$2.35 \cdot 10^7 s^{-1}$	$1.99 \cdot 10^7 s^{-1}$

Frequency domain identification

Both regular parts of $H(s)$ (3.23) and (3.26) have been identified. Then, the propagation function has been approximated exploiting the identified regular parts. This is shown in figg. (4.1), (4.2), (4.3), (4.4), (4.5), where the regular part obtained with the factorizing approach is indicated as [F] in the legend, whereas that one obtained with the subtracting approach is indicated as [S].
For the subtracting approach (definition (3.23)), both pure VF and VF+NLLS have been used. A good accuracy has been obtained with only 2 poles.

In order to study the accuracy, we define the error as the average value of the following rms percent relative errors:

$$\varepsilon(i,j) = 100\sqrt{\sum_{k=1}^{N_s} |H_{ij}(f_k) - \tilde{H}_{ij}(f_k)|^2 / \sum_{k=1}^{N_s} |H_{ij}(f_k)|^2} \tag{4.1}$$

where f_k are the N_s frequencies where the functions are computed. For the subtracting approach this error is 0.72% with a pure VF identification, and is

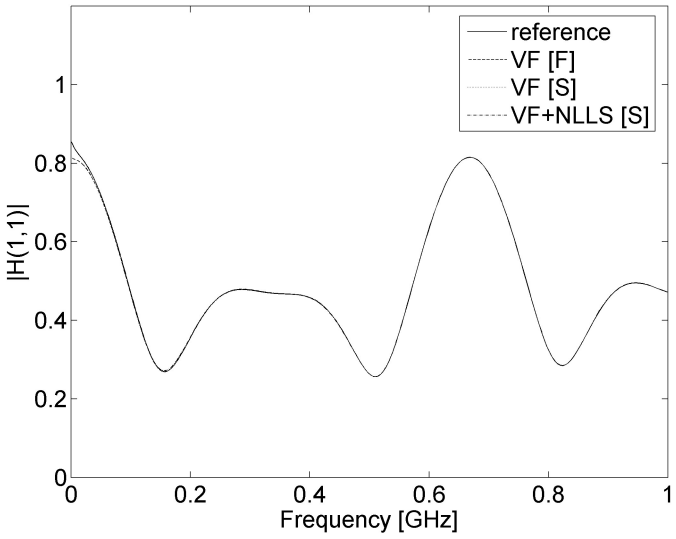

Figure 4.1: Interconnect 1 : identification of $|H_{11}|$

lower (0.45%) for VF+NLLS. For the factorizing approach (3.26), the error is 15.52%, mainly located at low frequencies, as shown in fig. (4.1).

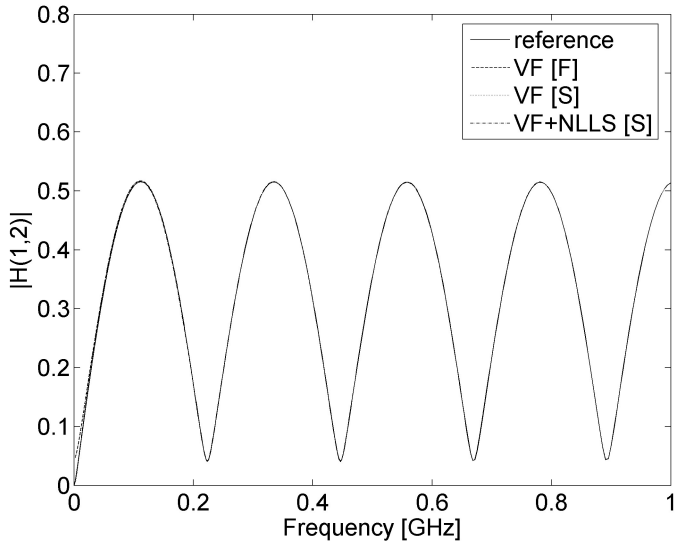

Figure 4.2: Interconnect 1 : identification of $|H_{12}|$

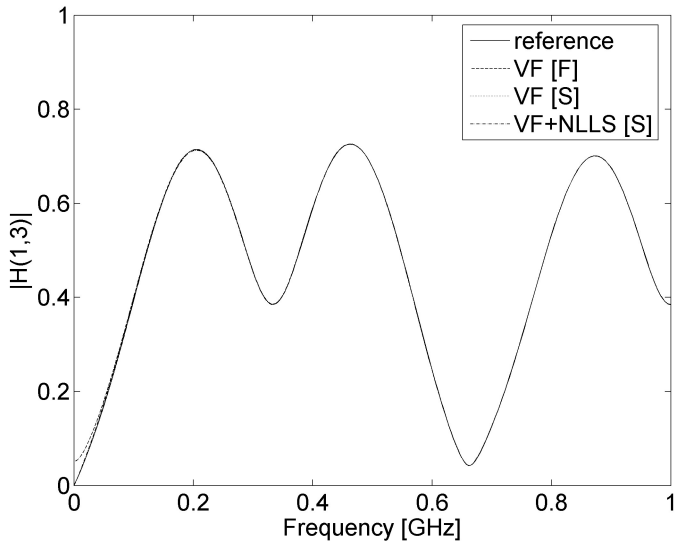

Figure 4.3: Interconnect 1 : identification of $|H_{13}|$

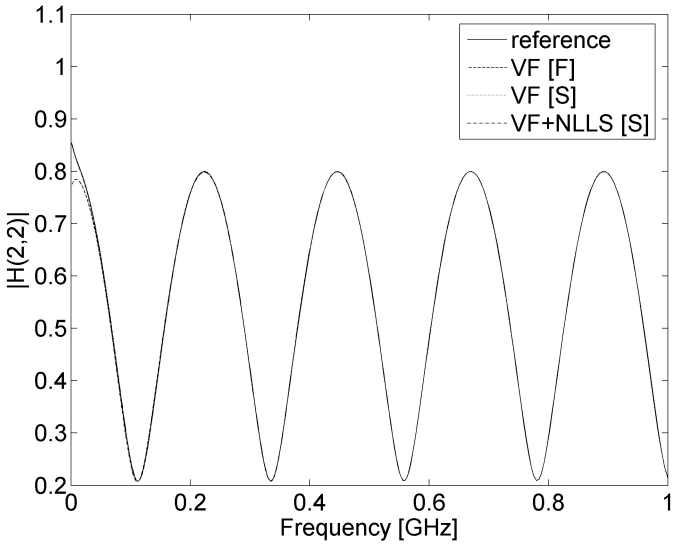

Figure 4.4: Interconnect 1 : identification of $|H_{22}|$

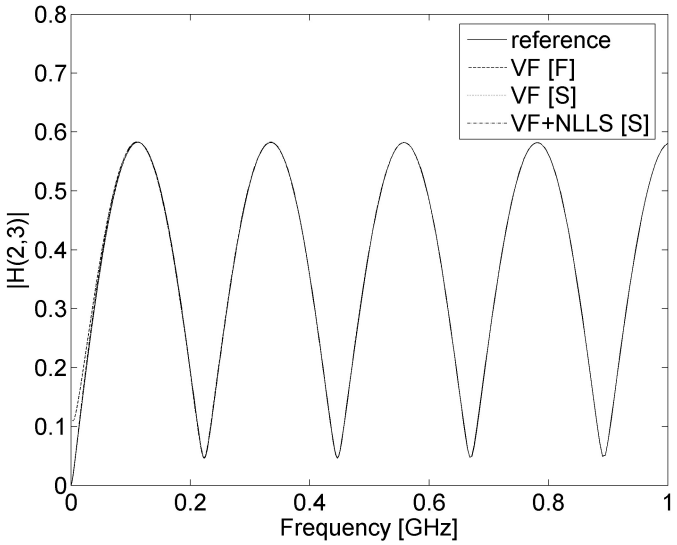

Figure 4.5: Interconnect 1 : identification of $|H_{23}|$

The particular shape of H components shown in figg. (4.1), (4.2), (4.3), (4.4), (4.5), due to the sensible difference in the delays, makes the numerical inversion of the overall propagation operator a very hard task. Obviously this problem is overcome when the method of characteristic is used.
Note that the cascade VF+NLLS may be used also for the factorizing approach (3.26). However, in this case the accuracy remain unvaried. This is due to

the different structural properties of the matrix to be identified, which in the factorizing case shows off-diagonal terms whose amplitude is order of magnitude smaller than the diagonal one.
As for the operator Y_{cr}, a 2 poles VF and VF+NLLS have been used. The corresponding errors, defined as above, are respectively 1.58% for VF and 0.69% for VF+NLLS.

Time domain analysis

As for the time domain analysis, we consider the line to be ended to linear loads. At the left end we assume the line 1 to be fed by a unit square voltage pulse of width $10^{-8}s$, in series with a 100Ω resistor, whereas both lines 2 and 3 are simply ended with two 100Ω resistors. The three line at the far-end are all terminations on 1 kΩ resistors.
Figure (4.6) shows the time-domain waveforms of a far-end crosstalk voltage: the approximated results obtained by means of the decomposition (3.23) and (3.26) are compared to the reference one, which is obtained through the convolution with the exact functions $Y_c(s)$ and $H(s)$. The errors, defined consistently to (4.1), are 0.69% for (3.23) and 0.74% for (3.26).

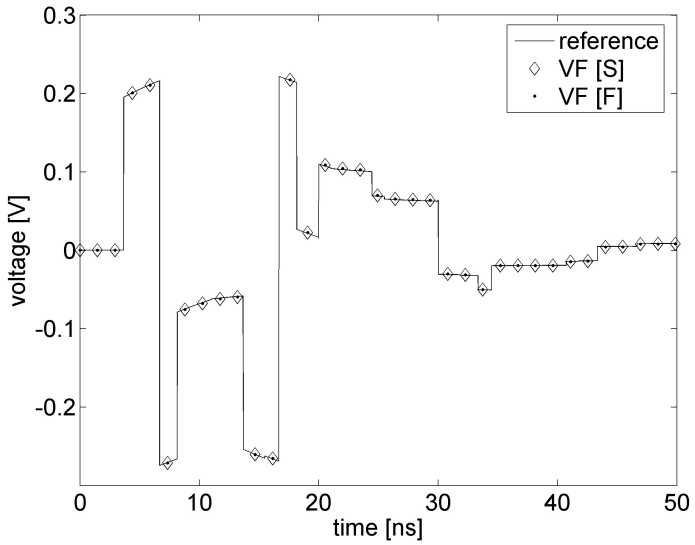

Figure 4.6: Interconnect 1 : far end crosstalk voltage v_{23} for case 1

4.2.2 Case study 2

The second case-study refers to a three-conductors TL (Mao and Kuh 1997 [63]) of 70 cm length, once again described by frequency-independent p.u.l. parameters

Table 4.3: Interconnect 2 : p.u.l. parameters

$R = \begin{pmatrix} 52 & 3.5 \\ 3.5 & 66 \end{pmatrix} \frac{\Omega}{m}$	$L = 10^{-9} \begin{pmatrix} 224.0 & 57.62 \\ 57.62 & 306.5 \end{pmatrix} \frac{H}{m}$
$G = 10^{-6} \begin{pmatrix} 0.98 & 0 \\ 0 & 0.98 \end{pmatrix} \frac{S}{m}$	$C = 10^{-12} \begin{pmatrix} 245.9 & -61.38 \\ -61.38 & 206.5 \end{pmatrix} \frac{F}{m}$

Table 4.4: Interconnect 2 : delay times and damping coefficients

	Mode 1	Mode 2
τ_i	0.498 ns	0.545 ns
μ_i	$1.08 \cdot 10^8 s^{-1}$	$1.24 \cdot 10^8 s^{-1}$

(4.3). The computed delay times T_i and damping coefficients μ_i are reported in (4.4): here the TEM modes propagate with quite the same velocity.

Frequency domain identification

Once again, the identification has been performed according to the definition given in (3.8), (3.23) and (3.26), with 4 poles for Y_{cr} and 6 poles for H_r, both further refined with the NLLS step.
As for Y_{cr}, a sensible fitting accuracy improvement is achieved with the cascade VF+NLLS. A typical gain in accuracy is shown in fig. (4.7) for the (1,2) entry. Similar accuracies are obtained for the other components. By using the average value of (4.1), we get for a 4-poles VF approach an error of 1.28% which reduces to 0.29% for a 4-poles VF+NLLS. As for the operator H_r, an accuracy of 4.25% is achieved with a 6-poles VF, which remains substantially the same (4.83%) for a 6-poles VF+NLLS.

Time domain analysis

A time domain analysis has been performed by considering the line connected at the near end to the same source and resistive loads as for Case 1, with respect to lines 1 and 2. Two different load conditions at the far-end are considered: first the line is terminated on its ideal characteristic impedance $Z_L = Y_c^{-1}$, then the mismatched load Z_L=diag(1,1) kΩ is considered. Figure (4.8) shows the near-end crosstalk voltage computed via a pure VF identification (4 poles for Y_{cr} and 6 poles for H_r), and by using the cascade VF+NLLS with the same number of poles. The errors in this waveform are 5.26% for VF and 2.76% for VF+NLLS. For the far-end crosstalk voltage we get the same order of accuracy, whereas for

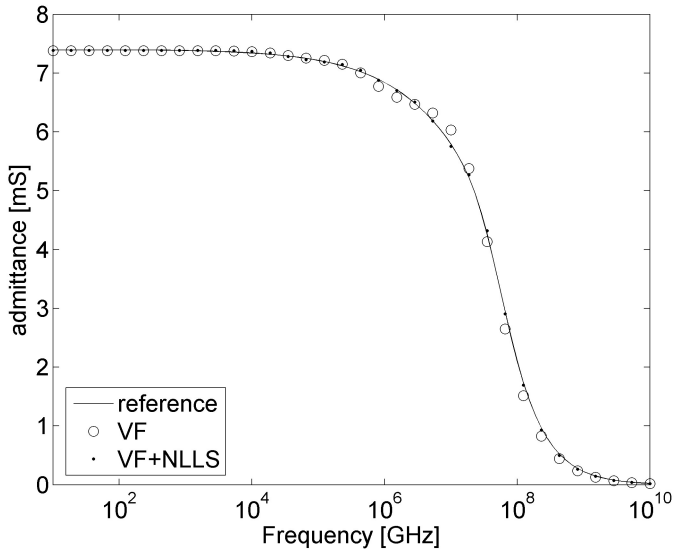

Figure 4.7: Interconnect 2 : identification of the magnitude of Y_{cr12}

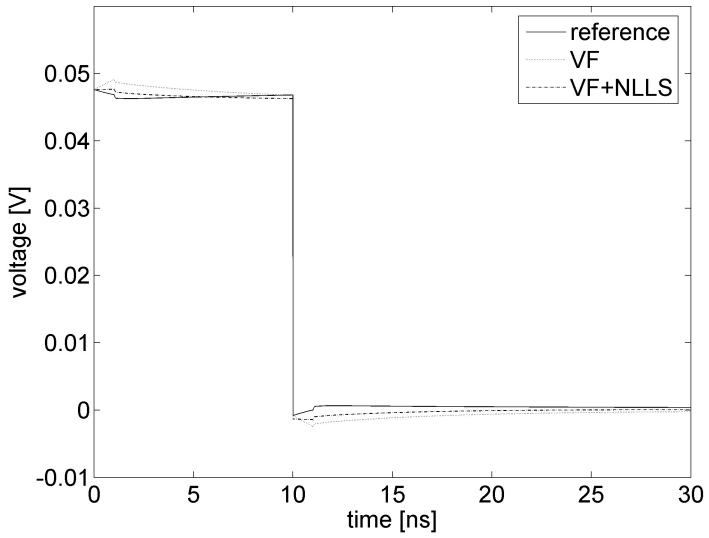

Figure 4.8: Interconnect 2 : near end crosstalk voltage of the active line, matched condition

the active line voltages we have a better accuracy, which is practically the same for the two identification procedures: 0.72% for VF and 0.82% for VF+NLLS. When the mismatched load is considered, there is a slight decrease of the accuracy. Figure (4.9) shows the far-end voltage of the active line: the errors are 2.34% for VF and 2.48% for VF+NLLS.

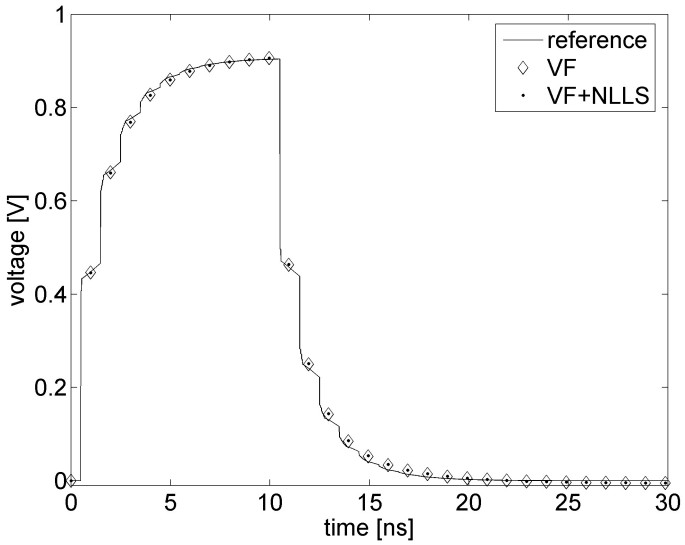

Figure 4.9: Interconnect 2 : far end crosstalk voltage of the active line, mismatched condition

4.2.3 Case study 3

The third case-study refers to a lossy coupled line with frequency-dependent parameters, given at certain frequency points. The data are reported in Ruehli et al (2002) [64] and here in tables (4.5) and (4.6), where the line is referred to as "Line 6". Here the line length is assumed to be 5 cm. The computed delay times T_i and damping coefficients μ_i are reported in (4.7): here the TEM modes propagate with quite the same velocity.

Frequency domain identification

For this case a 6 poles VF identification has been used to evaluate Y_{cr}, with a further NLLS step. Figure (4.10) shows the magnitude of the entry Y_{cr11}. The errors are 0.82% for VF and 0.65% for VF+NLLS. A 10 poles VF approximation has been used for identification of H_r, both with VF and VF+NLLS procedures. The errors on H are of the order of 10% for both procedures, which may be sensibly reduced by increasing the number of poles. Note that in this case only the factorizing approach (3.26) can be used: this is because with this kind of data eq. (3.20) only provides an approximation of the damping coefficients.

Time domain analysis

The time-domain simulations are performed by assuming the two near end terminals to be respectively connected with a unitary voltage step in series with a 100

Table 4.5: Interconnect 3 : p.u.l. parameters (R and L)

Frequency	R_{11}	R_{12}	R_{22}	L_{11}	L_{12}	L_{22}
0.0000E+00	1.1903E-4	1.9747E-6	1.1903E-4	5.7964E-3	1.6327-3	5.7964E-3
1.0000E-04	1.1922E-4	2.1100E-6	1.1922E-4	5.7373E-3	1.5939E-3	5.7373E-3
2.1500E-04	1.1978E-4	2.5357E-6	1.1978E-4	5.5629E-3	1.4669E-3	5.5629E-3
4.6400E-04	1.2133E-4	3.6863E-6	1.2133E-4	5.1299E-3	1.1224E-3	5.1299E-3
1.0000E-03	1.2370E-4	5.0714E-6	1.2370E-4	4.5856E-3	7.1098E-4	4.5856E-3
2.1500E-03	1.2609E-4	5.7029E-6	1.2609E-4	4.2299E-3	5.1188E-4	4.2299E-3
4.6400E-03	1.2847E-4	5.6902E-6	1.2847E-4	4.0633E-3	4.6542E-4	4.0633E-3
1.0000E-02	1.3310E-4	5.8278E-6	1.3310E-4	3.9975E-3	4.6151E-4	3.9975E-3
2.1500E-02	1.4722E-4	6.7940E-6	1.4722E-4	3.9385E-3	4.5665E-4	3.9385E-3
4.6400E-02	1.8349E-4	9.8021E-6	1.8349E-4	3.8339E-3	4.4825E-4	3.8339E-3
1.0000E-01	2.4997E-4	1.4318E-5	2.4997E-4	3.7130E-3	4.3855E-4	3.7130E-3
2.1500E-01	3.6067E-4	2.0543E-5	3.6067E-4	3.6095E-3	4.3152E-4	3.6095E-3
4.6400E-01	5.1958E-4	3.0331E-5	5.1958E-4	3.5293E-3	4.2701E-4	3.5293E-3
1.0000E+00	7.5879E-4	4.4306E-5	7.5879E-4	3.4744E-3	4.2353E-4	3.4744E-3
2.1500E+00	1.1014E-3	6.6335E-5	1.1014E-3	3.4372E-3	4.2128E-4	3.4372E-3
4.6400E+00	1.6241E-3	9.7411E-5	1.6241E-3	3.4120E-3	4.1977E-4	3.4120E-3
1.0000E+01	2.4029E-3	1.4139E-4	2.4029E-3	3.3936E-3	4.1869E-4	3.3936E-3
2.1500E+01	3.4585E-3	1.9669E-4	3.4585E-3	3.3818E-3	4.1808E-4	3.3818E-3
4.6400E+01	5.1625E-3	3.0437E-4	5.1625E-3	3.3735E-3	4.1757E-4	3.3735E-3
1.0000E+02	7.6153E-3	4.4942E-4	7.6153E-3	3.3678E-3	4.1717E-4	3.3678E-3

Ω, and with a 100 Ω resistor. The far end is terminated on the ideal characteristic impedance $Z_L = Y_c^{-1}$. Figures (4.11) and (4.12) show, respectively, the voltages computed at the far ends of the active and the victim lines. The errors in these waveforms are 0.42% for VF and 0.67% for VF+NLLS for the active line voltage. For the victim line we have a 0.14% error for VF and a 0.43% for VF+NLLS.

Table 4.6: Interconnect 3 : p.u.l. parameters (G and C)

Frequency	G_{11}	G_{12}	G_{22}	C_{11}	C_{12}	C_{22}
1.0000E-04	2.511793E-8	-3.387800E-9	2.711593E-8	1.362606	-1.702408E-1	1.362606
2.1500E-04	1.253419E-7	-1.565992E-8	1.253419E-7	1.362606	-1.702408E-1	1.362606
4.6400E-04	5.837550E-7	-7.293297E-8	5.837550E-7	1.362605	-1.702406E-1	1.362605
1.0000E-03	2.710696E-6	-3.386680E-7	2.710696E-6	1.362599	-1.702399E-1	1.362599
2.1500E-03	1.251506E-5	-1.563602E-6	1.251506E-5	1.362571	-1.702364E-1	1.362571
4.6400E-03	5.796317E-5	-7.241782E-6	5.796317E-5	1.362445	-1.702206E-1	1.362445
1.0000E-02	2.624262E-4	-3.278691E-5	2.624262E-4	1.361877	-1.701497E-1	1.361877
2.1500E-02	1.088212E-3	-1.359586E-4	1.088212E-3	1.359620	-1.698677E-1	1.359620
4.6400E-02	3.502414E-3	-4.375834E-4	3.502414E-3	1.353488	-1.691016E-1	1.353488
1.0000E-01	7.815921E-3	-9.765026E-4	7.815921E-3	1.345955	-1.681605E-1	1.345955
2.1500E-01	1.699811E-2	-2.123703E-3	1.699811E-2	1.340388	-1.674650E-1	1.340388
4.6400E-01	3.987868E-2	-4.982348E-3	3.987868E-2	1.333386	-1.665901E-1	1.333386
1.0000E+00	7.860268E-2	-9.820432E-3	7.860268E-2	1.326305	-1.657054E-1	1.326305
2.1500E+00	1.648290E-1	-2.059334E-2	1.648290E-1	1.321384	-1.650906E-1	1.321384
4.6400E+00	3.921098E-1	-4.898928E-2	3.921098E-1	1.314875	-1.642774E-1	1.314875
1.0000E+01	7.985241E-1	-9.976572E-2	7.985241E-1	1.307774	-1.633902E-1	1.307774
2.1500E+01	1.699677	-2.123536E-1	1.699677	1.302361	-1.627139E-1	1.302361
4.6400E+01	3.844613	-4.803368E-1	3.844613	1.294859	-1.617767E-1	1.294859
1.0000E+02	6.187092	-7.730007	6.187092	1.287259	-1.608271E-1	1.287259

Table 4.7: Interconnect 3 : delay times and damping coefficients

	Mode 1	Mode 2
τ_i	0.498 ns	0.545 ns
μ_i	$1.08 \cdot 10^8 s^{-1}$	$1.24 \cdot 10^8 s^{-1}$

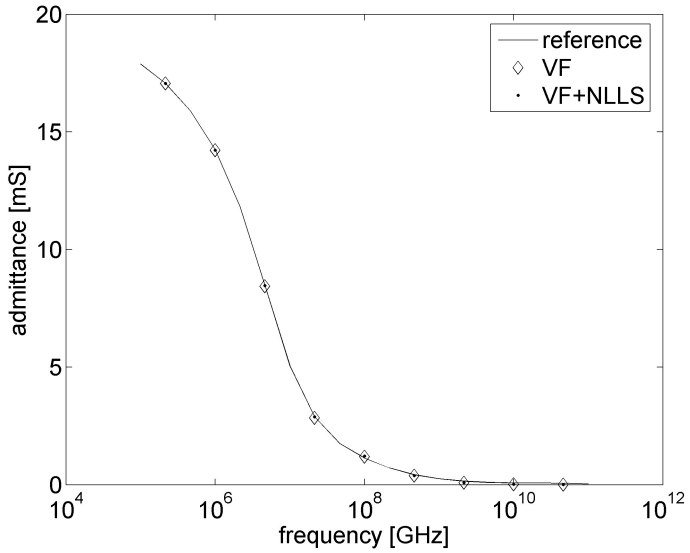

Figure 4.10: Interconnect 3 : identification of the magnitude of Y_{cr11}

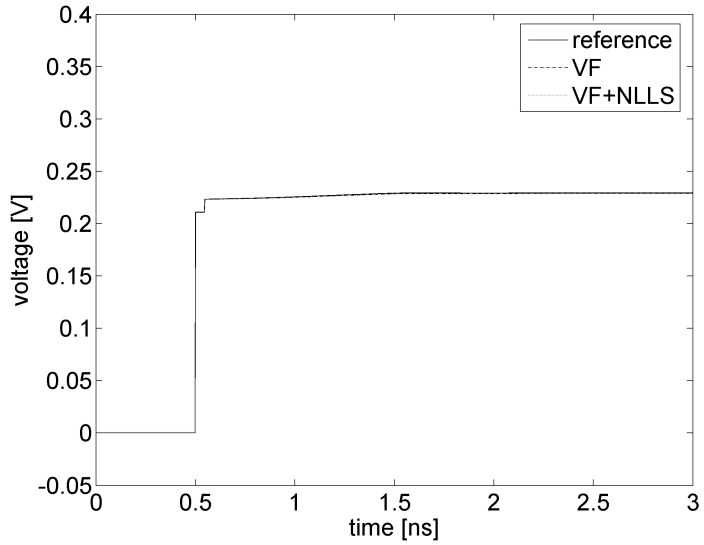

Figure 4.11: Interconnect 3 : voltage at far end of the active line

4.3 Analysis of electromagnetic transients in transmission cables

In this section we consider the application of the previously described identification methodologies to transmission cables. As test case, a 10 km long single underground cable is considered.

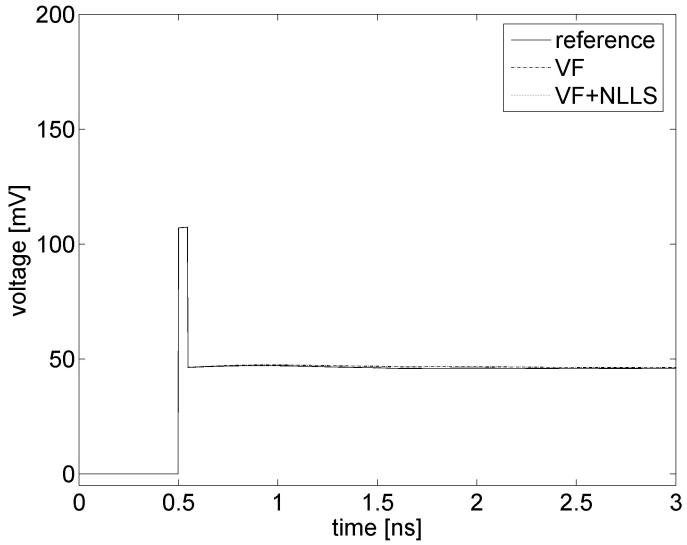

Figure 4.12: Interconnect 3 : voltage at far end of the victim line

Figure (4.13) shows the fitting of the coaxial mode using previously described approaches. It is seen that both combined procedure and phase reconstruction gives a more accurate result than the asymptotic fitting based procedure. Figure

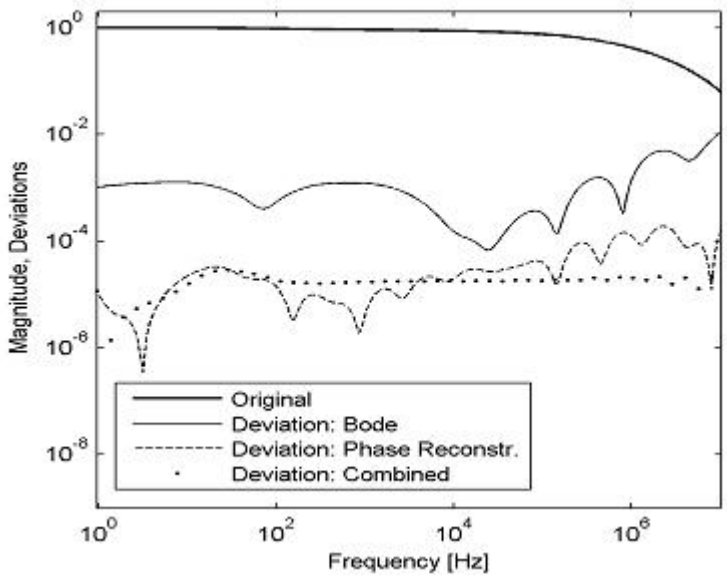

Figure 4.13: Underground cable : identification of the coaxial mode (N=16)

(4.14) shows the fitting of the ground mode. Also in this case, both combined procedure and phase reconstruction gives a higher accuracy than the asymptotic

fitting based procedure. The figure also shows that the combined procedure gives the best result in terms of accuracy for this case.
After that each modal component of $H(s)$ have been identified, the phase domain fitting of $H(s)$ has to be performed. We use the approach provided by the ULM. Since phase domain fitting uses only poles and time delays of the identified modes, the accuracy achieved on modes is only partially related to the accuracy achievable on the phase domain fitting. In this case, we found that both phase reconstruction and combined procedure give similar results when performing the phase domain fitting, although the ground mode (fig. 4.14) was best fitted through the combined procedure.

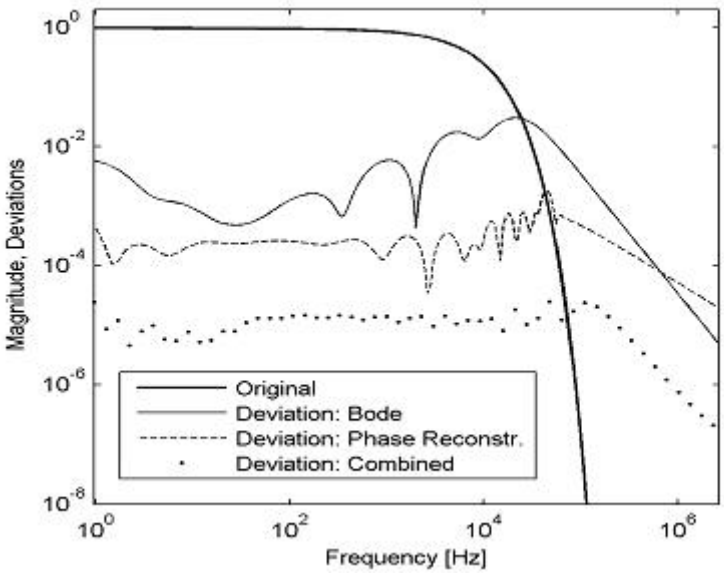

Figure 4.14: Underground cable : identification of the ground mode (N=16)

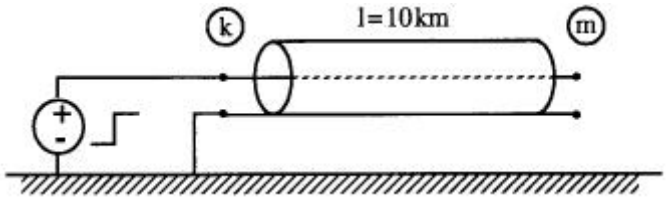

Figure 4.15: Underground cable : open circuit step response

Identified reduced order models have been tested in a typical time domain simulation: the evaluation of an open circuit step responses, fig. (4.15).
Figures (4.16) and (4.17) show the exact induced sheath voltage (calculated by the Fourier Method given by Gustavsen et al 1995 [65]), together with deviations

from such solution when each modal component of $H(s)$ and the characteristic admittance matrix $Y_c(s)$ are identified with N poles. In particular, fig. (4.16)

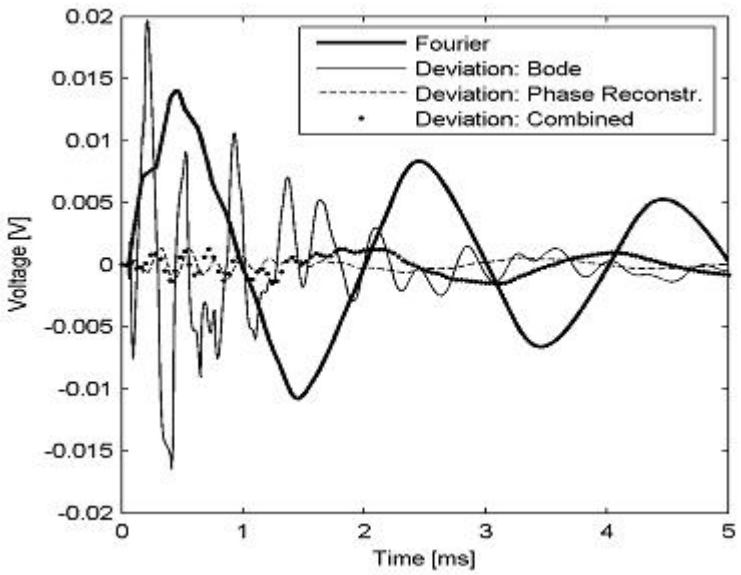

Figure 4.16: Underground cable : induced sheath voltage (N=12)

shows that the Bode fitting approach gives a completely wrong result with $N = 12$, since its deviation is greater than the exact solution. Deviations from exact solution of phase reconstruction approach and combined procedure with $N = 12$ are very similar and satisfactory. Instead, fig. (4.17) shows that the Bode fitting approximation gives a satisfactory result with $N = 12$, but still less accurate than other procedures in the interval $[0, 1.5ns]$. Deviations from exact solution of phase reconstruction approach and combined procedure are still very similar. Figure (4.18) shows the core voltage at far end. It is seen that all the procedures give a satisfactory result with only $N = 8$ poles, although the Bode fitting is still less accurate than others.

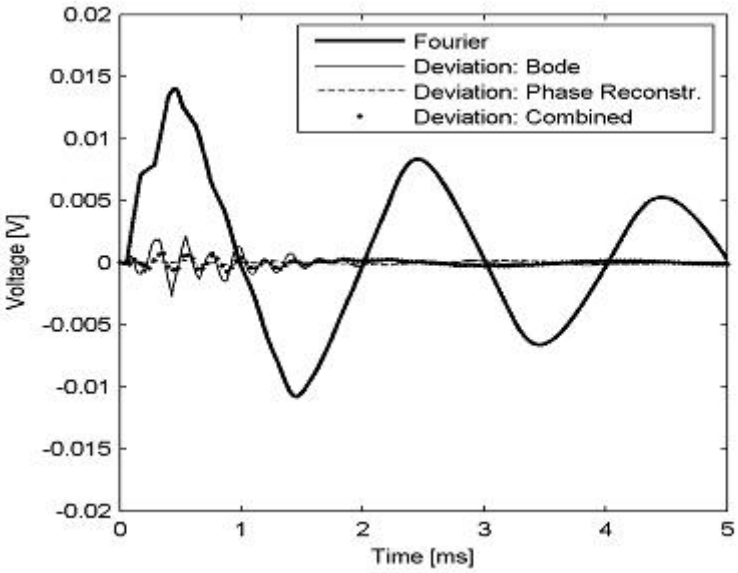

Figure 4.17: Underground cable : induced sheath voltage (N=16)

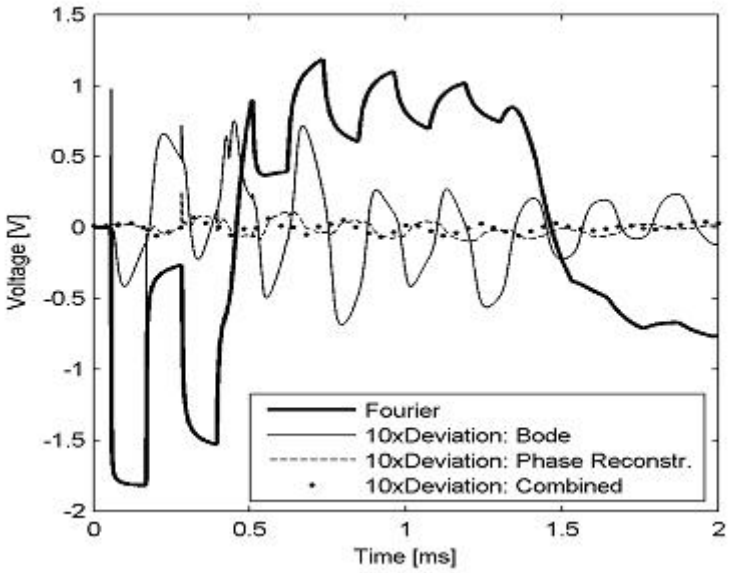

Figure 4.18: Underground cable : core voltage at far end (N=8)

4.4 Modelling of interconnects in non-TEM conditions

Accurate modelling of electrical interconnects is required in the design of the modern electronic systems to address several signal integrity issues.
In this section, we consider the issue of macromodeling for a large class of elec-

trically long interconnects, made of two perfectly conducting parallel wires embedded in a homogeneous dielectric, operating in non-TEM conditions.
In many practical VLSI applications, the bandwidth of signals carried by the electrical interconnects extends to frequency ranges where the quasi-TEM hypothesis of propagation does no longer hold. In such cases, the transmission line model is inadequate to catch those high-frequency effects, like radiation and dispersion, which actually affect the system performance.
Electrically long interconnects operating in non-TEM conditions have to be characterized in the frequency domain through a transfer matrix (i.e. impedance, admittance or scattering parameters). This requires a full-wave analysis, which may be performed by means of different approaches. In [45], Miano and Villone (2005) exploited a general surface integral formulation of Maxwell equations to derive a numerical solution of the problem. The approach has been implemented in a computer code named SURFCODE. Nevertheless, being the considered interconnects long and uniform, a one-dimensional model is still accurate. This allows a more efficient description based on a suitable extended transmission line model. Such a kind of model, named "Enhanced Transmission Line" (ETL) model, has been proposed in [66] by Maffucci et al (2004). It can describe correctly the behaviour of the structure also in the frequency ranges where the smallest characteristic wavelength approaches the conductor separation. Basic concepts concerning the full-wave electromagnetic formulation, needed to both mentioned approaches will be briefly recalled in the next section.
Starting from the simulated port responses, the identification of a reduced order model is pursued through some least square algorithm, for instance the VF algorithm. The second fundamental issue addressed is the passivity enforcement on the identified reduced model.

4.4.1 Challenges in macromodeling of long interconnects

Electrically long interconnects described through the transmission line model, can be efficiently modelled in the time-domain by the popular Method of Characteristics (MoC), which describes the line by means of the characteristic admittance and the propagation function. Qualitative information on such a model allows the analytical extraction of the irregular terms of these functions (such as the delays involved in the propagation function). In this way, the rational approximation of the remainders of both describing operators is almost trivial, being them smooth functions [52].
When the physics of the propagation does not enable the use of the MoC, macromodels have to be derived from a characterization given as transfer function matrix, typically made of non-smooth frequency responses. Furthermore, propagation delays are not extracted and handled analytically, therefore mutual responses are non-minimum phase shift functions. This demands to use high orders

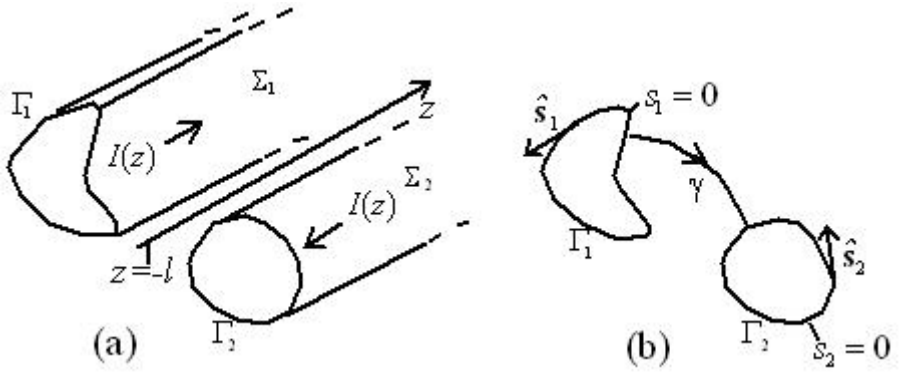

Figure 4.19: Non-TEM interconnect : (a) schematic representation of the geometry; (b) tranverse cross section

for achieving good approximations.
Second issue concerns the possibility that the identified macromodel violates the passivity constraint in some frequency bands. Since the electromagnetic model adopted is known as inconsistent in some frequencies band, passivity violations arise in the original data (Maffucci et al 2005 [67]). These violations will also affect the macromodel.
In order to show where the mentioned problem originates, we need to introduce some aspects of the electromagnetic model.

Let us consider an interconnect of length $2l$, made of two perfectly conducting parallel wires with arbitrary cross-sections, embedded in a homogeneous dielectric, see figure (4.4.1).
The electromagnetic field can be represented, in the frequency domain, through the potentials A and φ:

$$E = -j\omega A - \nabla\varphi, B = \nabla \times A. \tag{4.2}$$

The expressions relating these potentials to current and charge distributions are not uniquely defined until a gauge condition has been fixed. When the Lorentz gauge condition:

$$\nabla \cdot A(P) + j\frac{\omega}{c^2}\varphi(P) = 0 \tag{4.3}$$

is assumed valid, such expressions become decoupled.
The surface charge distribution $\sigma = \sigma(r)$ and surface current distribution $J_s = J_s(r)$ are determined by imposing the charge conservation law and the constitutive equations for perfect conductors (the tangential component of E vanishes on the conductor surfaces $\sum_1, \sum_2$).
Since the goal is the characterization of the interconnect as a multiport circuit, the contributions given to the potentials A and φ by the currents and charges lying on the physical devices that will be connected to the structure, cannot be

taken into account. As a result of this approximation, potentials will not exactly verify the Lorenz gauge condition (4.3). This has been recognized as cause of passivity violation bands for the impedance matrix Z [67].

4.4.2 Passivity enforcement

The analysis developed in [67], identified bands where the real part of the self impedance Z_{self} takes negative values. Here, we do not exploit such kind of physics-based analysis, preferring to enforce the passivity constraint directly on the whole identified transfer matrix. In fact, even setting $Re\{Z_{self}\} = 0$ at those frequencies where $Re\{Z_{self}\} < 0$, data do not become consistent, since this is a weaker condition than PR condition (2.1).
Best results for the passivity enforcement have been found by applying the method of Hamiltonian perturbation [38].

4.4.3 Test cases

We consider a case-study given by Chiariello et al (2005) in [34]. It refers to two square conductors with a= 1 mm, b = 1 mm, h_c = 10 mm, and a length of $2l$ = 100 mm. Impedances matrices $Z(s)$ of such interconnects have been obtained through a computer code based on the ETL model. Before starting the identification of the reduced model, the sign of eigenvalues of ReZ have been checked, finding slight violations distributed over large frequency bands. These violations also results in the reduced model identified through the VF algorithm. Therefore, a proper correction to the original fitting is needed. We apply the method recalled in section (2.2.2), which has been implemented in the public domain computer code IdEM.
Figures (4.21) and (4.22) show the identification of the rational approximations of Z_{11} and Z_{12}. It can be seen that accuracy is substantially unchanged after correcting the passivity violations. Figures (4.23) and (4.24) show the correction given to the eigenvalues of $Re\{Z\}$.

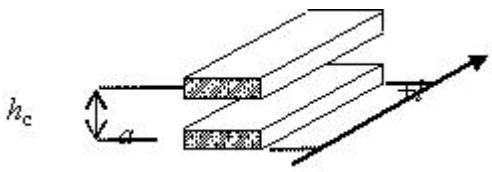

Figure 4.20: Non-TEM interconnect : Reference geometry for the considered case studies.

Table 4.8: Non-TEM interconnect : bands (f_1,f_2) of passivity violations of the identified macromodel (N=14)

f_1	f_2	min. eig. of $Re(Z)$
6.816e9	5.729e9	-114.26
5.716e9	4.334e9	-14.28
4.262e9	2.893e9	-8.44
2.837e9	1.447e9	-4.22
1.415e9	6.015e8	-1.22
2.398e9	1.947e6	-0.006

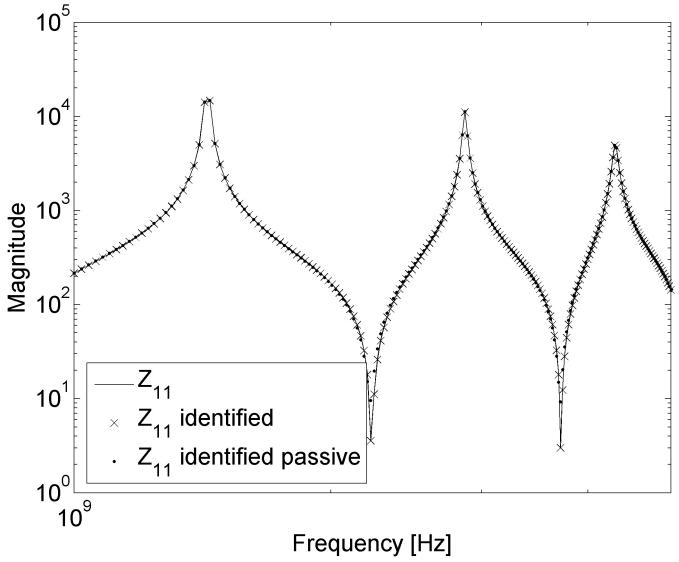

Figure 4.21: Non-TEM interconnect: identification of the magnitude of Z_{11} (N=14)

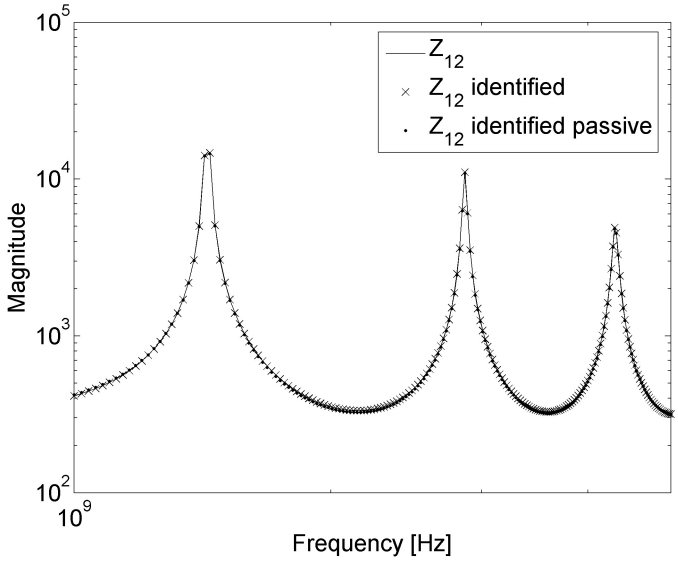

Figure 4.22: Non-TEM interconnect: identification of the magnitude of Z_{12} (N=14)

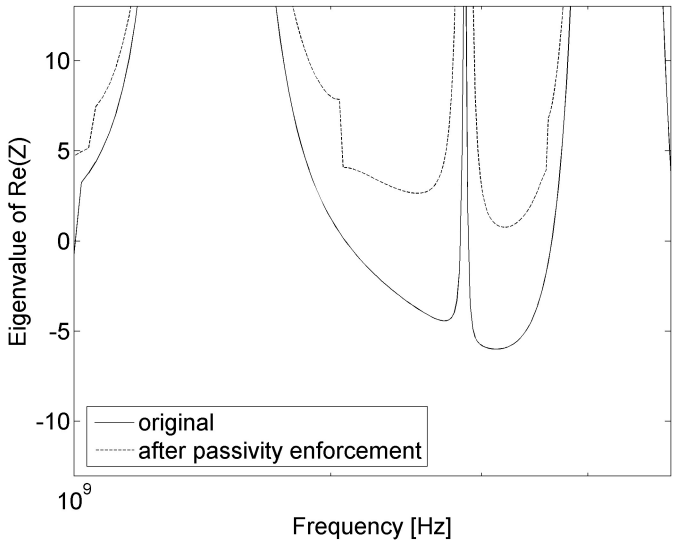

Figure 4.23: Non-TEM interconnect: passivity enforcement on the first eigenvalue

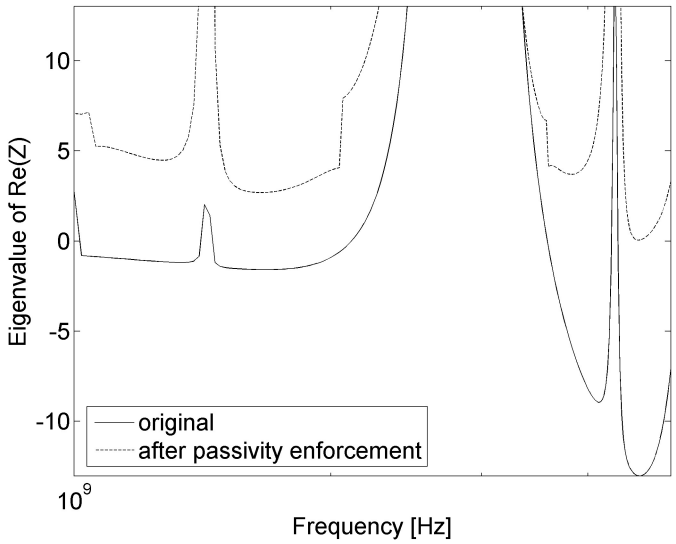

Figure 4.24: Non-TEM interconnect: passivity enforcement on the second eigenvalue

Bibliography

[1] E. C. Levy. Complex curve fitting. *IRE Transaction on Automatic Control*, AC-4:37–43, May 1959. [cited at p. 6]

[2] C. K. Sanathanan and J. Koerner. Transfer function synthesis as a ratio of two complex polynomials. *IEEE Transaction on Automatic Control*, AC-8:56–58, January 1963. [cited at p. 6, 9]

[3] A. K. Shaw. Optimal design of digital iir filters by model-fitting frequency response data. *IEEE Transaction on Circuits and Systems-II. Analog and Digital Signal Processing*, 42(11):702–710, November 1995. [cited at p. 6]

[4] B. Gustavsen and A. Semlyen. Rational approximation of frequency domain responses by vector fitting. *IEEE Transaction on Power Delivery*, 14(3):1052–1061, July 1999. [cited at p. 6, 9, 10, 14, 22, 40]

[5] B.Gustavsen, G. Irwin, R. Mangelrad, D. Brandt, and K. Kent. Transmission line models for the simulation of interaction phenomena between parallel ac and dc overhead lines. *Proceedings of International Conference on Power System Transients (IPST)*, 1999. [cited at p. 7]

[6] R. Fletcher. *Practical Methods of Optimization*. Wiley. [cited at p. 8, 33]

[7] J.N. Brittingham, E.K. Miller, and J.L. Willows. Pole-extraction from real-frequency information. *Proceedings of IEEE*, 68(2), February 1980. [cited at p. 9]

[8] Rong Gao, Y.S. Mekonnen, W.T. Beyene, and J.E. Schutt-Aine. Black-box modeling of passive systems by rational function approximation. *IEEE Transactions on Advanced Packaging*, 28(2):209–215, May 2005. [cited at p. 9, 10, 30]

[9] W. Hendrickx and T. Dhaene. A discussion of "rational approximation of frequency domain responses by vector fitting". *IEEE Transactions on Power Systems*, 21(1):441–443, February 2006. [cited at p. 9]

[10] B. Gustavsen. Improving the pole relocating properties of vector fitting. *IEEE Transactions on Power Delivery*, 21(3):1587–1592, July 2006. [cited at p. 9, 10, 16]

[11] D. Deschrijver and T. Dhaene. Broadband macromodelling of passive components using orthonormal vector fitting. *Electronics Letters*, 41(21):1160–1161, October 2005. [cited at p. 10]

[12] D. Deschrijver and T. Dhaene. Rational modeling of spectral data using orthonormal vector fitting. *Proceedings of 9th IEEE Workshop on Signal Propagation on Interconnects*, pages 111–114, May 2005. [cited at p. 10]

[13] G. Antonini, D. Deschrijver, and T. Dhaene. A comparative study of vector fitting and orthonormal vector fitting techniques for emc applications. *IEEE International Symposium on Electromagnetic Compatibility*, 1:6–11, August 2006. [cited at p. 10]

[14] D. Deschrijver, B. Haegeman, and T. Dhaene. Orthonormal vector fitting: A robust macromodeling tool for rational approximation of frequency domain responses. *IEEE Transactions on Advanced Packaging*. accepted for future publication. [cited at p. 10]

[15] L. Zhao J.L. Prince M. Elzinga, K.L. Virga. Pole-residue formulation for transient simulation of high-frequency interconnects using householder ls curve-fitting techniques. *IEEE Transactions on Advanced Packaging*, 23(2):142–147, May 2000. [cited at p. 10]

[16] J.L. Prince M. Elzinga, K.L. Virga. Improved global rational approximation macromodeling algorithm for networks characterized by frequency-sampled data. *IEEE Transactions on Microwave Theory and Techniques*, 48(9):1461–1468, September 2000. [cited at p. 10]

[17] W.T. Beyene and J.E. Schutt-Aine. Efficient transient simulation of high-speed interconnects characterized by sampled data. *IEEE Trans. Comp., Packag., Manuf. Technol. B*, 21(1):105–114, January 1998. [cited at p. 11]

[18] W.T. Beyene. Improving time-domain measurements with a network analyzer using a robust rational interpolation technique. *IEEE Transactions on Microwave Theory and Techniques*, 49(3):500–508, March 2001. [cited at p. 11]

[19] Zhongyuan Zhang, Guishu Liang, Xiang Cui, and Maolin Wu. A high frequency transfer function model of potential transformer in gis. *IEEE 3rd International Symposium on Electromagnetic Compatibility*, pages 186–189, May 2002. [cited at p. 14]

[20] Hendrik W. Bode. *Network Analysis and Feedback Amplifier Design.* D. VAN NOSTRAND COMPANY, Inc., 250 Fourth Avenue, 1945. [cited at p. 14]

[21] J.R. Marti. Accurate modelling of frequency-dependent transmission lines in electromagnetic transient simulations. *IEEE Transactions on Power Apparatus and Systems*, PAS-101(1):147–157, 1982. [cited at p. 14, 52, 56, 60]

[22] B. Gustavsen L. De Tommasi. Low order transmission line modeling by modal decomposition and minimum phase shift fitting. *Proceedings of 10th IEEE Workshop on Signal Propagation on Interconnects*, 9-12 May 2006. [cited at p. 14, 51]

[23] B. Gustavsen. Application of vector fitting to high frequency transformer modeling. *Proceedings of International Conference on Power System Transients*, paper 9d-2:157–174, 28 September - 2 October 2003. New Orleans. [cited at p. 18]

[24] R. Neumayer, A. Stelzer, F. Haslinger, and R. Weigel. On the synthesis of equivalent-circuit models for multiports characterized by frequency-dependent parameters. *IEEE Transactions on Microwave Theory and Techniques*, 50(12):2789–2796, December 2002. [cited at p. 21, 22]

[25] I. Maio I.S. Stievano S. Grivet Talocia, F. .Canavero. Reduced order macromodeling of complex multiport interconnects. *URSI General Assembly, Maastricht, Belgium*, 19-23 August 2002. [cited at p. 22]

[26] B. Gustavsen. Computer code for rational approximation of frequency dependant admittance matrices. *IEEE Transaction on Power Delivery*, 17(4), October 2002. [cited at p. 22, 24, 40]

[27] A. Semlyen B. Gustavsen. A robust approach for system identification in the frequency domain. *IEEE Transactions on Power Delivery*, 19(3):1167–1173, July 2004. [cited at p. 22, 23, 24]

[28] P. Russer T. Mangold. Full-wave modeling and automatic equivalent-circuit generation of millimeter-wave planar and multilayer structures. *IEEE Transactions on Microwave Theory and Techniques*, 47(6):851–858, June 1999. [cited at p. 23]

[29] W. Cauer. Ideale transformatoren und lineare transformationen. *Elektr. Nachr. Technol.*, 9:157–174, 1932. [cited at p. 23]

[30] M. de Magistris; L. De Tommasi. An identification technique for macromodeling of long interconnects. *Proceedings of 9th IEEE Workshop on Signal Propagation on Interconnects*, pages 185–188, 10-13 May 2005. [cited at p. 23, 24]

[31] A. Maffucci G. Miano L. Corti, M. de Magistris. Efficient time-domain simulation of lossy multiconductor lines with non-linear loads. *1999 IEEE International Symposium on Electromagnetic Compatibility*, 1:440–445, 2-6 August 1999. [cited at p. 24]

[32] B. Gustavsen. Frequency-dependent modeling of power transformers with ungrounded windings. *IEEE Transactions on Power Delivery*, 19(3):1328–1334, July 2004. [cited at p. 29]

[33] B. Gustavsen. Wide band modeling of power transformers. *IEEE Transactions on Power Delivery*, 19(1):414–422, January 2004. [cited at p. 29]

[34] G. Miano F. Villone W. Zamboni A.G. Chiariello, A. Maffucci. Signal integrity analysis of high-speed interconnects through a full-wave transmission line model. *Proceedings of 9th IEEE Workshop on Signal Propagation on Interconnects*, pages 47–50, 10-13 May 2005. [cited at p. 29, 79]

[35] A. Semlyen B. Gustavsen. Enforcing passivity for admittance matrices approximated by rational functions. *IEEE Transactions on Power Systems*, 16(1):97–104, February 2001. [cited at p. 30, 31]

[36] A. Semlyen A. Feijoo J. Cidras F.A.M. Cipparrone, B. Gustavsen. Discussion of "enforcing passivity for admittance matrices approximated by rational functions". *IEEE Transactions on Power Systems*, 16(4):954–955, November 2001. [cited at p. 30]

[37] A. Semlyen B. Gustavsen. Closure to discussion of "enforcing passivity for admittance matrices approximated by rational functions". *IEEE Transactions on Power Systems*, 16(4):955–955, November 2001. [cited at p. 30]

[38] S. Grivet-Talocia. Passivity enforcement via perturbation of hamiltonian matrices. *IEEE Transactions on Circuits and Systems I: Regular Papers*, 51(9):1755–1769, September 2004. [cited at p. 30, 32, 34, 79]

[39] B.D.O. Anderson and S. Vongpanitlerd. *Network analysis and synthesis*. Prentice-Hall, Englewood Cliffs, New Jersey, 1973. [cited at p. 30]

[40] L.M. Silveira C.P. Coelho, J. Phillips. A convex programming approach for generating guaranteed passive approximations to tabulated frequency-data. *IEEE Transactions on Computer-Aided Design of Integrated Circuits and Systems*, 23(2):293–301, February 2004. [cited at p. 32]

[41] K. Sivaprasad K. Chamberlin, K. Komisarek. A method-of-moments solution to the twisted-pair transmission line. *IEEE Transactions on Electromagnetic Compatibility*, 37(1):121–126, February 1995. [cited at p. 33]

[42] J.E. Schutt-Aine. High-frequency characterization of twisted-pair cables. *IEEE Transactions on Communications*, 49(4):598–601, April 2001. [cited at p. 33]

[43] F. Maradei S. Caniggia. Spice-like models for the analysis of the conducted and radiated immunity of shielded cables. *IEEE Transactions on Electromagnetic Compatibility*, 46(4):606–616, November 2004. [cited at p. 33]

[44] K. Sivaprasad K. Chamberlin, K. Komisarek. A method-of-moments solution to the twisted-pair transmission line. *IEEE Transactions on Electromagnetic Compatibility*, 37(1):121–126, February 1995. [cited at p. 33, 34]

[45] Miano G. and Villone F. A surface integral formulation of maxwell equations for topologically complex conducting domains. *IEEE Transactions on Antennas and Propagation*, 53(12):4001–4014, February 2005. [cited at p. 34, 77]

[46] R.F. Harrington A.R. Djordjevic, T.K. Sarkar. Time-domain response of multiconductor transmission lines. *Proceedings of the IEEE*, 75(6):743–764, June 1987. [cited at p. 39]

[47] C. R. Paul. *Analysis of Multiconductor Transmission Lines*. Wiley, New York, 1994. [cited at p. 39]

[48] C. R. Paul. Decoupling the multiconductor transmission line equations. *IEEE Transactions on Microwave Theory and Techique*, 44:1429–1440, August 1996. [cited at p. 39]

[49] G. Miano A. Maffucci. Irregular terms in the impulse response of a multiconductor lossy transmission line. *IEEE Transactions on Circuits and Systems I: Fundamental Theory and Applications*, 46(7):788–805, July 1999. [cited at p. 39]

[50] S. Lin and E. S. Kuh. Transient simulation of lossy interconnects based on the recursive convolution formulation. *IEEE Transactions on Circuits and Systems I*, 39:879–892, November 1992. [cited at p. 40]

[51] T. Blazeck C. Gordon and R. Mittra. Time-domain simulation of multiconductor transmission lines with frequency-dependent losses. *IEEE Transactions on Computer-Aided Design*, CAD-11:1372–1387, 1992. [cited at p. 40]

[52] A. Maffucci G. Miano. *Transmission lines and lumped circuits*. Academic Press, San Diego, California 92101-4495, USA, 2001. [cited at p. 40, 41, 44, 45, 77]

[53] A.E. Ruehli A. Dounavis M.S. Nakhla I.M. Elfadel, Hao-Ming Huang. A comparative study of two transient analysis algorithms for lossy transmission lines with frequency-dependent data. *IEEE Transactions on Advanced Packaging*, 25(2):143–153, May 2002. [cited at p. 40]

[54] A.E. Ruehli F. Canavero I.M. Elfadel S. Grivet-Talocia, Hao-Ming Huang. Transient analysis of lossy transmission lines: an efficient approach based on the method of characteristics. *IEEE Transactions on Advanced Packaging*, 27(1):45–56, February 2004. [cited at p. 40, 45]

[55] M. Tartibi A. Morched, B. Gustavsen. A universal model for accurate calculation of electromagnetic transients on overhead lines and underground cables. *IEEE Transactions on Power Delivery*, 14(3):1032–1038, July 1999. [cited at p. 43, 46, 47, 49]

[56] A. Maffucci G. Miano M. de Magistris, L. De Tommasi. Accurate identification of long interconnects with the generalized method of characteristics. *Proceedings of the 16th International Zurich Symposium on Electromagnetic Compatibility*, 13-18 February 2005. [cited at p. 45]

[57] H.V. Nguyen L.M. Wedepohl and G.D. Irwin. Frequency-dependent transformation matrices for untransposed transmission lines using newton-raphson method. *IEEE Transactions on Power Systems*, 11(3):1538–1546, August 1996. [cited at p. 47]

[58] L. Marti. Simulation of transients in underground cables with frequency-dependent modal transformation matrices. *IEEE Transactions on Power Delivery*, 3(3):1099–1110, July 1988. [cited at p. 47]

[59] A. Semlyen B. Gustavsen. Simulation of transmission line transients using vector fitting and modal decomposition. *IEEE Transactions on Power Delivery*, 13(2):605–614, April 1998. [cited at p. 47]

[60] Editor in Chief : A.D. Poularikas. *The Transforms and Application Handbook*. CRC Press and IEEE Press, 1996. [cited at p. 48]

[61] B. Gustavsen. Time delay identification for transmission line modeling. *Proceedings of 8th IEEE Workshop on Signal Propagation on Interconnects*, pages 103–106, 9-12 May 2004. [cited at p. 49, 51, 55, 60]

[62] The Math Works Inc. *Optimization Toolbox User's Guide - version 2*. 2000. [cited at p. 55]

[63] E.S. Kuh Jun-Fa Mao. Fast simulation and sensitivity analysis of lossy transmission lines by the method of characteristics. *IEEE Transactions on*

Circuits and Systems I: Fundamental Theory and Applications, 44(5):391–401, May 1997. [cited at p. 66]

[64] H.M. Huang A.E. Ruehli, A.C. Cangellaris. Three test problems for the comparison of lossy transmission line algorithms. *Electrical Performance of Electronic Packaging*, pages 347–350, 21-23 October 2002. [cited at p. 69]

[65] T. Henriksen B. Gustavsen, J. Sletbak. Calculation of electromagnetic transients in transmission cables and lines taking frequency dependent effects accurately into account. *IEEE Transactions on Power Delivery*, 10(2):1076–1084, April 1995. [cited at p. 74]

[66] F. Villone A. Maffucci, G. Miano. An enhanced transmission line model for conducting wires. *IEEE Transactions on Electromagnetic Compatibility*, 46(4):512–528, November 2004. [cited at p. 77]

[67] F. Villone A. Maffucci, G. Miano. An enhanced transmission line model for conductors with arbitrary cross sections. *IEEE Transactions on Advanced Packaging*, 28(2):174–188, May 2005. [cited at p. 78, 79]

List of Symbols and Abbreviations

Abbreviation	Description	Definition
VF	Vector Fitting algorithm	page 6
MIMO	Multi Input Multi Output systems	page 7
SK	Sanathanan-Koerner algorithm	page 9
RFA	Rational Function Approximation algorithm	page 9
MBPE	Model Based Parameter Estimation algorithm	page 9
SVF	Symmetric Vector Fitting	page 15
PR	Positive Real	page 30
BR	Bounded Real	page 30
LMIs	Linear Matrix Inequalities	page 32
IdEM	Identification of Electrical Macromodel computer code	page 34
MoC	Method of Characteristics	page 39
ULM	Universal Line Model	page 46
ETL	Enhanced Transmission Line model	page 77

List of Figures

List of Tables